Supporting Information for

LOBSTAHS: An Adduct-Based Lipidomics Strategy for Discovery and Identification of Oxidative Stress Biomarkers

James R. Collins[*,†,‡], Bethanie R. Edwards[†,‡,§] Helen F. Fredricks[‡], and Benjamin A. S. Van Mooy[‡]

[†]Massachusetts Institute of Technology/Woods Hole Oceanographic Institution Joint Program in Oceanography, Woods Hole, MA 02543, USA

[‡]Department of Marine Chemistry and Geochemistry, Woods Hole Oceanographic Institution, Woods Hole, MA 02543, USA

***Corresponding author:** E-mail: james.r.collins@aya.yale.edu

Table of Contents

EXPERIMENTAL SECTION

Instructions for Obtaining Software and Data Referenced in the Text. The current release of the LOBSTAHS package can be compiled using R devtools from source files maintained at https://github.com/vanmooylipidomics/LOBSTAHS. A readme file and R vignette in the repository contain step-by-step installation and operation instructions. The fully processed *Phaeodactylum tricornutum* dataset is available from https://github.com/vanmooylipidomics/PtH2O2lipids as the R data package PtH2O2lipids. Both packages are provided under the MIT License. Auxiliary R scripts necessary for pre-processing of data are maintained at https://github.com/vanmooylipidomics/LipidomicsToolbox. Raw files for the *P. tricornutum* dataset may be downloaded at ftp://ftp.whoi.edu/pub/science/MCG/gbmf/VanMooy/OxylipinAnalysis; metadata for the dataset are provided at http://www.whoi.edu/page.do?pid=133616&tid=282&cid=192529/. Scripts used for statistical analysis of the *P. tricornutum* dataset and to produce the figures presented in the text are available from https://github.com/jamesrco/LipidomicsDataViz.

Conversion of .raw Data Files to .mzXML Format. After acquiring data from the mass spectrometer, we employed a short, custom R script ("Exactive_full_scan_process_ms1+.R") to automate three functions of the msConvert[1] command-line tool. The script first converts all Thermo .raw files in a given dataset to the open-source .mzXML format, which is used by many chromatographic alignment and peak picking applications. It then converts the profile-mode mass spectral data in each file to a series of centroids. Finally, the script automates the extraction of the positive and negative ion mode full scan events from each sample into separate files. In the Exactive instrument configuration described in the text, the full scan events from the two ion modes appeared in each data file as the first and third scan events at each time point, respectively. (The second and fourth scan events at each time point were the positive and negative mode AIF scans.) The extraction and separation of scans from the two ion modes was necessary to accomplish subsequent analysis using the pipeline. In our analysis of the *P. tricornutum* dataset, we omitted from this step two blanks and data from two samples collected at the 4 h timepoint (one of two replicates from each of the 0 μM and 150 μM H_2O_2 treatments) because of an unexpected shift in chromatography that rendered the data incompatible with our analysis.

Sample Injection, Chromatography and ESI Source Settings. 20 μL injections of sample were made onto a C8 Xbridge HPLC column (particle size 5 μm, length 150 mm, width 2.1 mm; Waters Corp., Milford, MA, USA). Eluent A consisted of water with 1% 1M ammonium acetate and 0.1% acetic acid. Eluent B consisted of 70% acetonitrile, 30% isopropanol with 1% 1M ammonium acetate and 0.1% acetic acid. Gradient elution was performed with the following program (total run time 30 min) at a constant flow rate of 0.4 mL min^{-1}: 45% A for 1 min to 35% A at 4 min, then from 25% A to 11% A at 12 min, then to 1% A at 15 min with an isocratic hold until 25 min, and finally back to 45% A for 5 min column equilibration. ESI source settings were: Spray voltage, 4.5kV (+), 3.0 kV (-); capillary temperature, 150°C; sheath gas and auxiliary gas, both 21 (arbitrary units); heated ESI probe temperature, 350°C.

Mass Spectrometer Acquisition Settings. Mass data were collected on a ThermoFisher Exactive Plus Orbitrap instrument in full scan (FS) and all-ion-fragmentation modes (AIF) while alternating between positive and negative ion modes. A scan range of 150-1500 *m/z* was used for all modes in sequence (FT MS positive full scan, FT MS positive AIF, FT MS negative full scan, and FT MS negative AIF, respectively). The S-lens RF level was set to 85.00. Mass resolution was set to the maximum possible value of 140,000 (FWHM at *m/z* 200) for both FS and AIF. This mass resolution setting corresponded to an observed resolution of 75,100 at the *m/z* (875.5505) of our internal standard, DNP-PE. The observed resolution at *m/z* 1269.0952, that of the compound in the screened dataset with the highest molecular weight (TAG 76.6 +4O), was 41,100. Using these settings, we obtained between 8 and 14 MS scans across a typical peak.

Procedures Used for Weekly and Real-Time Calibration of the Exactive. The mass spectrometer was calibrated weekly in both positive and negative ion modes by infusing calibration mixes available from ThermoFisher Scientific. Low-level eluent contaminants were also utilized as lock masses, providing real-time recalibration; C16:0 (255.23295) and C18:0 (283.26425) fatty acids were used in negative ion mode, while a polysiloxane (536.16537) and phthalate (391.28429) were used in positive ion mode. At least one of the lock masses was found during each positive and negative full scan event.

Script for Pre-Processing Data in xcms and CAMERA. We implemented xcms and CAMERA using the script "prepOrbidata.R," a version of which is available under the MIT License at https://github.com/vanmooylipidomics/LipidomicsToolbox. Users can modify the script as necessary. We used the R package IPO to optimize settings for xcms and CAMERA, obtaining the parameter values given in Table S5. We used these parameter values to obtain the results presented in the text.

Determination of Retention Time Window Data. The retention time (RT) window data in Table S4 were obtained primarily from authentic standards for representative compounds of each parent lipid class under the chromatographic conditions described in the text. Observations of various lipids in environmental samples allowed us to consider additional species. While LOBSTAHS applies the retention time data contained in Table S4 as a default, detailed instructions and an example data table are included in the onboard documentation for use with retention time data for other chromatographic methods. As for the adduct ion hierarchy data, retention time data for ox-IPL are inherited from the unoxidized parent molecule. By default, LOBSTAHS expands the retention time window for each lipid class by 20% of its given width to account for (1) shifts in retention time that may occur during

chromatographic alignment with xcms and (2) slight variations in retention time that distinguish the different positional (i.e., regio-) isomers of the same parent lipid.[2,3] This window can be narrowed or expanded with user input.

Analysis of Positive Ionization Mode *P. tricornutum* Data Using xcms, CAMERA, and LOBSTAHS. To examine the effect of oxidative stress on the *P. tricornutum* lipidome, we applied the LOBSTAHS workflow (Scheme 1) to a dataset assembled from only positive mode data files. We confined our analysis to the positive mode data because intact polar lipids (IPL), the primary targets of both reactive oxygen species (ROS) and lipoxygenase-mediated enzymatic transformations induced by H_2O_2, are most amenable to analysis in positive ion mode. The specific workflow and parameter values we applied to the dataset in xcms, CAMERA, and LOBTAHS are given in Table S5. We elected to apply all three optional filters to the data in LOBSTAHS.

Choice of Matching Tolerance. To account for variability in performance expected from natural samples, we used a 2.5 ppm mass uncertainty tolerance when matching against the databases. This tolerance was one order of magnitude more conservative than the 0.22 ppm mass uncertainty we observed with authentic standards (Table 1 and Table S6), yet considerably more restrictive than the various default standards used for matching in other recently introduced metabolomics applications.[4,5] When combined with HPLC separation and the high mass resolution of the Exactive, the 2.5 ppm tolerance still allowed us to assign distinct identities to isobaric masses.

Statistical Analysis and Visualization of the *P. tricornutum* Lipidome. LOBSTAHS workflow is designed to facilitate examination of relative changes in the abundances of lipids in a given dataset, not to enable absolute quantification of specific analytes or direct comparisons between datasets. With this in mind, the annotated output from LOBSTAHS was used to calculate the relative abundances of *P. tricornutum* lipidome constituents present in the 0 and 150 μM H_2O_2 treatments at 24 h. The analysis was performed as follows:

1. First, using the script "PtH2O2_mz-rt_plots.R," we extracted from the processed dataset a subset of "high confidence" assignments to be used in all subsequent analyses (i.e., assignments annotated with codes C1 or C2a and having no identified structural isomers or isobars; Figure 1a and symbols with darkest tones in Figures S2-S10). The remaining putative assignments we classified as "moderate confidence," indicating that the underlying features satisfied the hierarchy rules fundamentally yet imperfectly (symbols with lighter tones in Figures S2-S10). The peak areas of the high confidence assignments were normalized to data for an internal standard (DNP-PE). We then further restricted our analysis to only those compounds still present in two or more samples. ("PtH2O2_mz-rt_plots.R" and the other scripts referenced in the Supplemental Information are available from https://github.com/jamesrco/LipidomicsDataViz)

2. Using the script "PtH2O2_heatmap_sigclust.R," peak areas of the remaining assignments were then scaled using a level approach according to [6]. Each peak area, x_i, was divided by the average peak area of that compound across the dataset, x_{avg}, to obtain a normalized peak area, $\tilde{x}_i$:

$$\tilde{x}_i = \frac{x_i}{x_{avg}}$$

   Values of $\tilde{x}_i$ were then used in the steps described below to represent the relative abundances of the compounds present in each sample.

3. When the same compound appeared in duplicates of the same experimental treatment, values of $\tilde{x}_i$ were averaged. Since subsequent statistical analysis required $\log_2$ transformation of the data and many hierarchical clustering functions cannot use values of 0 or "NA" as inputs, all values of $\tilde{x}_i$ equal to 0 were replaced with 10^{-6}.

4. The heatmaps and dendrogram in Figures 2 and S11 were then generated from this subset of relative abundances using the R packages gplots[7] and clustsig[8]. Similarity profile analysis[9] was then used to cluster the molecular species in the subset according to their degree of covariation. The groups of lipidome components identified by this similarity profile analysis are presented in Table S8. Following this analysis, the heatmaps in Figures 2 and S11 was reordered and the dendrogram was rotated such that the order of compounds in both figures is from most upregulated in the 150 μM H_2O_2 treatment to most downregulated. The groups from the similarity profile analysis (Table S8) were categorized by the general response of their components to H_2O_2 treatment at 150 μM H_2O_2: 101 groups contained a total of 562 compounds more abundant in the 150 μM treatment (i.e., upregulated), 70 groups contained a total of 308 compounds less abundant in the 150 μM treatment

(i.e., downregulated), and 11 groups together contained 26 components whose abundance was not significantly different between the two treatments ($P \leq 0.01$).

SUPPLEMENTARY DISCUSSION

Fatty Acid Chain Elongation also Evident in Lipids Localized to other Cell Compartments. In addition to observations of fatty acid chain elongation in lipids typical of the chloroplast, significant elongation was also observed in moieties of phosphatidylethanolamine (PE) that were upregulated upon treatment with 150 μM H_2O_2. When lipids typical of the chloroplast (DGDG, SQDG, MGDG, and PG), endoplasmic reticulum (PC, PG, PE), and mitochondrion (PE and PG) were considered separately[10], we found that lipids with longer chain fatty acids were upregulated in mitochondria but not in the endoplasmic reticulum (Table S9). While our analysis suggested that oxidative stress in *P. tricornutum* resulted in a global shift toward lipids with longer chain fatty acids, the opposite lipidomic response was observed for *P. tricornutum* under nitrogen stress.[11] Nitrogen stress resulted in a decrease in both eicosapentaenoic (EPA; 20:5) and docosahexaenoic (DHA; 22:6) acids and a shift toward shorter chain length palmitic (16:0) and palmitoleic (16:1) acids.[11] We do not view the data we obtained using LOBSTAHS as incompatible with these findings; instead, the result suggests that different sources of stress upon the cell can induce specific and distinct signatures in the lipidome of *P. tricornutum*.

No Overall Increase Observed in Lipidome Oxidation State. We found no statistically significant differences in either the peak area allocated to oxidized lipid moieties or in the fraction of unique compounds identified as oxidized (Table S9; calculations not shown). One explanation for this finding is that the cultures were not sampled soon enough after treatment with H_2O_2 to observe oxidation of the lipidome before a rapid antioxidant response was induced in the organism. By 4 hours, the first timepoint at which the experiment was sampled, it is not unreasonable to expect that repair of much of the initial oxidative damage would already have been underway via upregulation of a suite of enzymatic and non-enzymatic plant antioxidant defense mechanisms.[12,13] In *Arabidopsis thaliana*, the lipidomic response to wounding, another source of oxidative stress, was nearly instantaneous; concentrations of several intact oxidized lipid species increased by as much three orders of magnitude within 15 minutes after the treatment was applied.[14]

SUPPLEMENTARY FIGURES

Figure S1. Extracted ion chromatogram (*m/z* 500-1500; positive ion mode) from a *P. tricornutum* sample treated with 150 μM H_2O_2. Spectra were acquired under the MS and HPLC conditions described in the text. Text annotations show prominent identifiable features and retention time ranges of some different lipid classes.

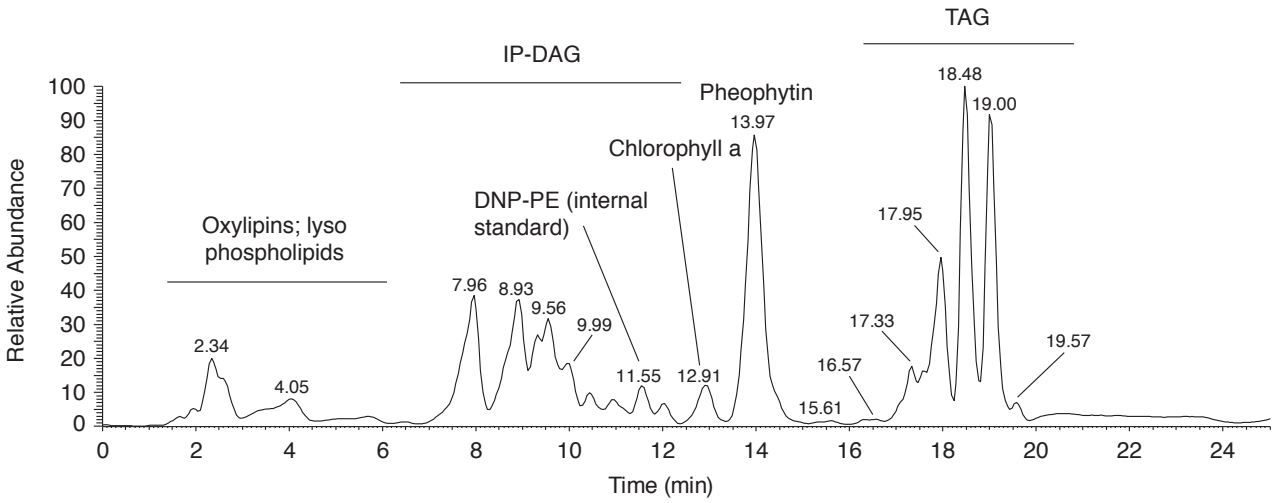

Figures S2-S10. Oxidized and intact species of nine classes of lipid identified in the *P. tricornutum* dataset after 24 hours in (a) the control (0 μM H_2O_2) and (b) 150 μM H_2O_2 treatments. Figures S2-S10 show species of, respectively, DGCC, DGDG, DGTS & DGTA, MGDG, PC, PE, PG, SQDG, and TAG. Shading indicates the degree of confidence in the identification, while symbols indicate the degree of oxidation by addition of one or more oxygen atoms. Excluded are those compounds having an odd total number of acyl carbon atoms, according to the reasoning described in the text; this exclusion is an optional, user-electable LOBSTAHS screening feature. Where practical, a text annotation indicates the number of acyl carbon atoms and double bonds in each compound. Data are presented for a single experiment with two technical replicates.

[a] Darkest tones indicate high and moderate confidence IDs for which no structural isomers or isobars were detected; these are compounds annotated with codes "C1," "C2a," or "C2b" in the LOBSTAHS workflow illustrated in Scheme 1.

[b] ≥ 1 structural isomer of an adduct of this compound is present in dataset (Scheme 1, code C3f).

[c] Adduct ion of ≥ 1 other compound is an isobar of the dominant adduct of this compound; i.e., *m/z* of the adducts are ≤ the 2 ppm match tolerance used in initial assignments (Scheme 1, code C3c).

[d] ≥ 1 structural isomer and ≥ 1 competing assignment of second type both present.

[e] Compounds of which multiple regioisomers were identified in single sample, indicating possible oxidation of the same parent molecule at different structural positions.

[f] General direction of movement within *m/z* versus RT plot for a given lipid class and oxidation state.

Figure S2

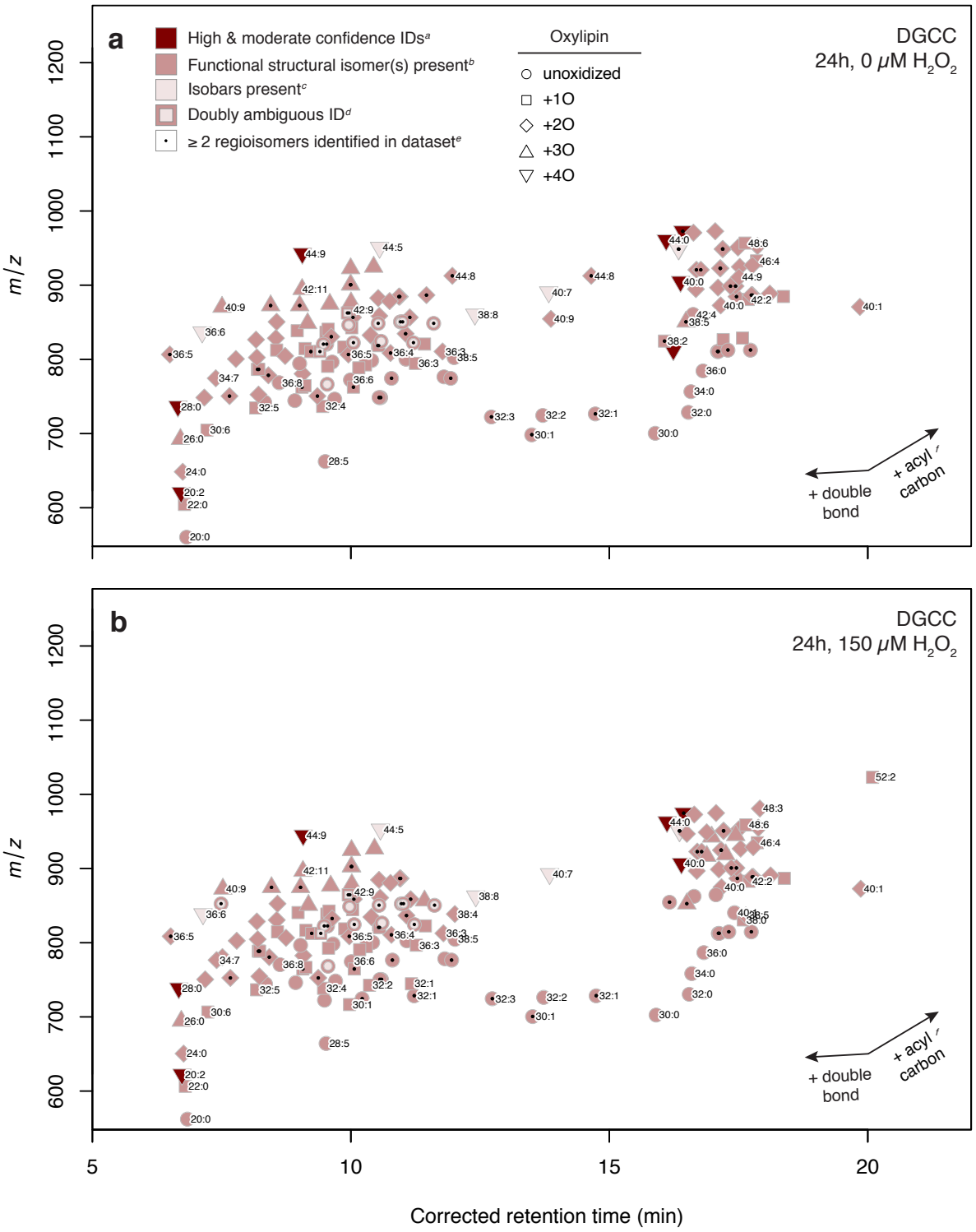
a
High & moderate confidence IDs[a]
Functional structural isomer(s) present[b]
Isobars present[c]
Doubly ambiguous ID[d]
≥ 2 regioisomers identified in dataset[e]
Oxylipin
unoxidized
+1O
+2O
+3O
+4O
DGCC
24h, 0 μM H2O2
b
DGCC
24h, 150 μM H2O2
+ double bond
+ acyl carbon
m/z
Corrected retention time (min)

Figure S3

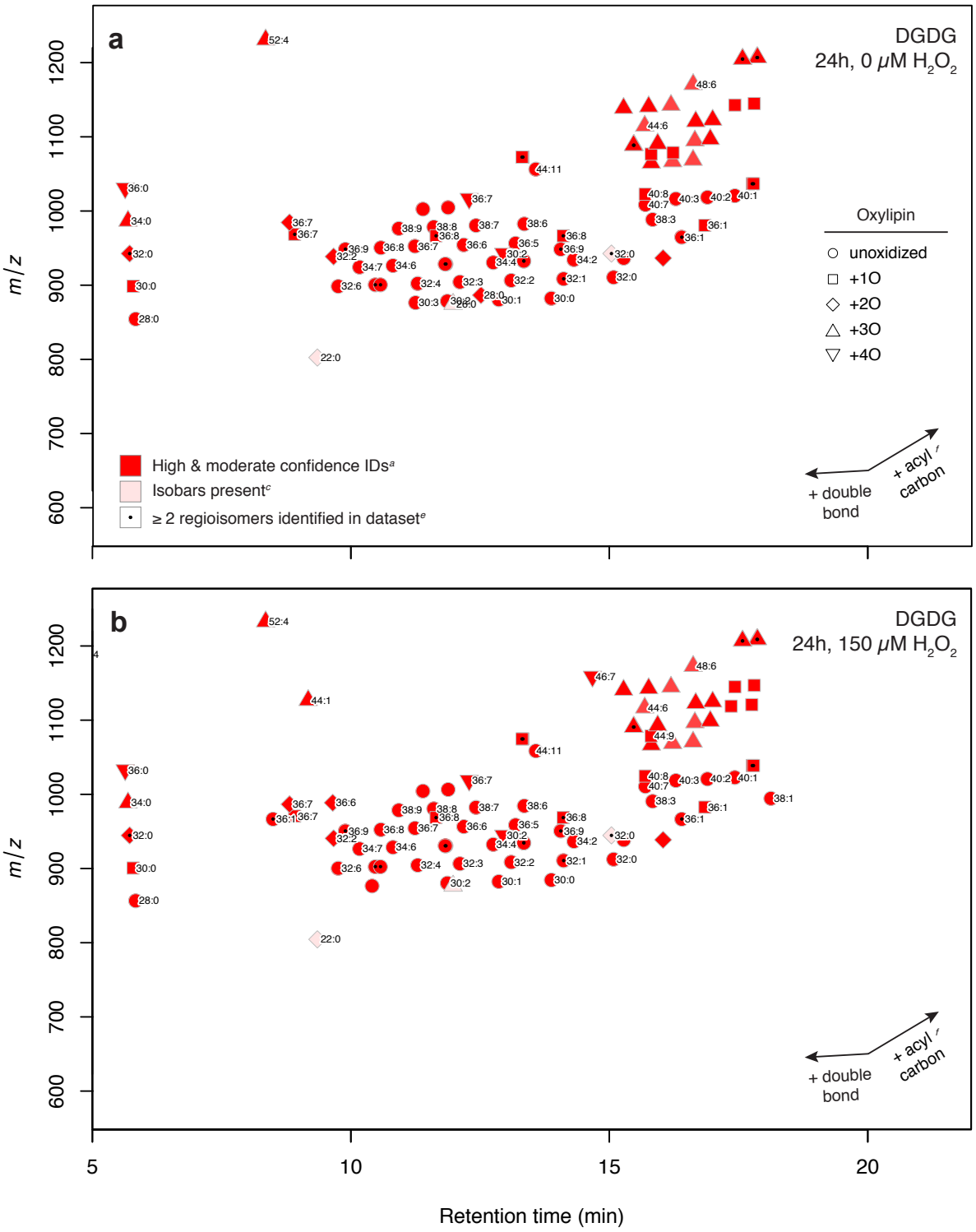
a
DGDG
24h, 0 μM H2O2
Oxylipin
unoxidized
+1O
+2O
+3O
+4O
High & moderate confidence IDs[a]
Isobars present[c]
≥ 2 regioisomers identified in dataset[e]
+ double bond
+ acyl carbon
b
DGDG
24h, 150 μM H2O2
m/z
Retention time (min)

Figure S4

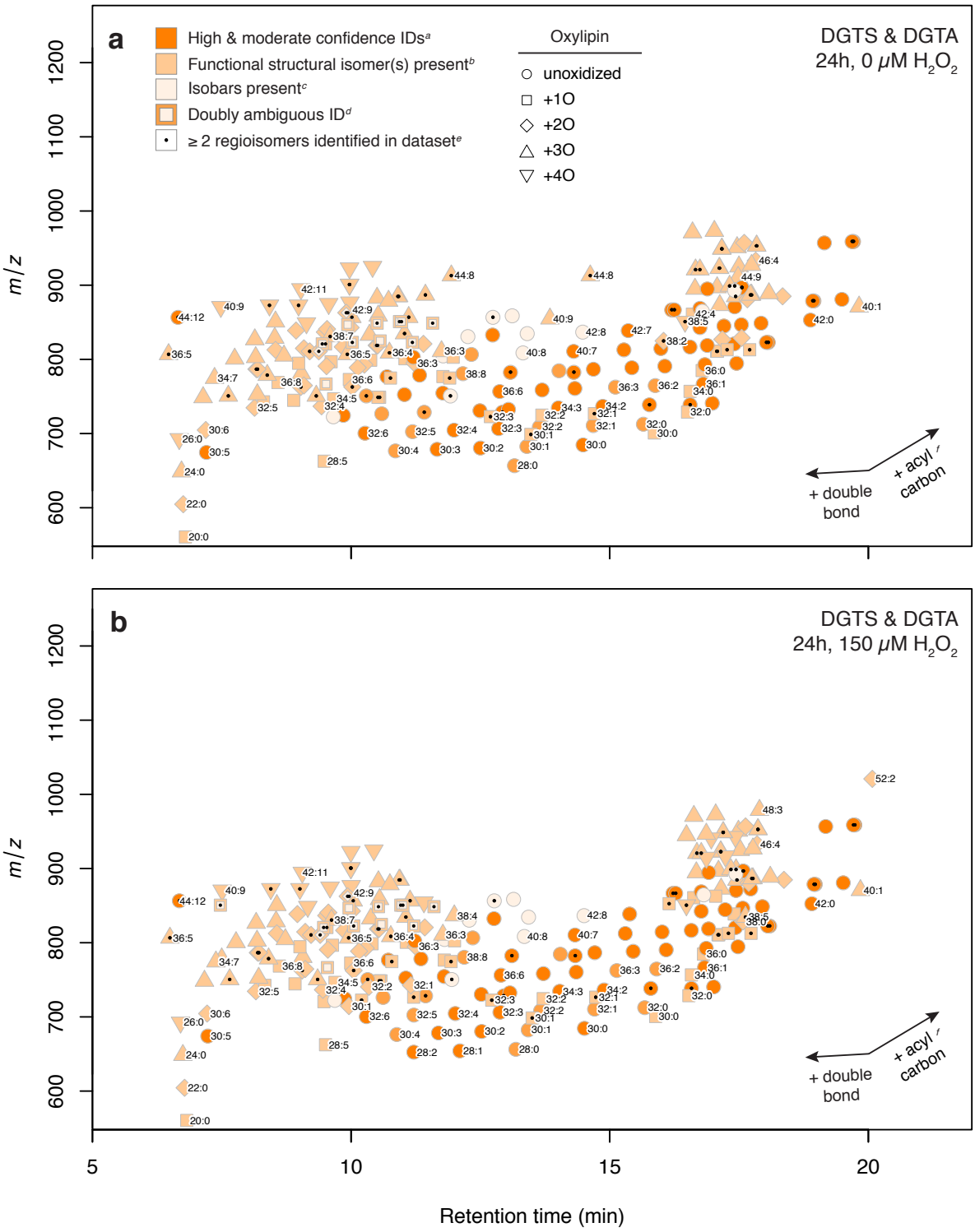
a
High & moderate confidence IDs[a]
Functional structural isomer(s) present[b]
Isobars present[c]
Doubly ambiguous ID[d]
≥ 2 regioisomers identified in dataset[e]
Oxylipin
unoxidized
+1O
+2O
+3O
+4O
DGTS & DGTA
24h, 0 μM H2O2
+ double bond
+ acyl carbon
b
DGTS & DGTA
24h, 150 μM H2O2
m/z
Retention time (min)

Figure S5

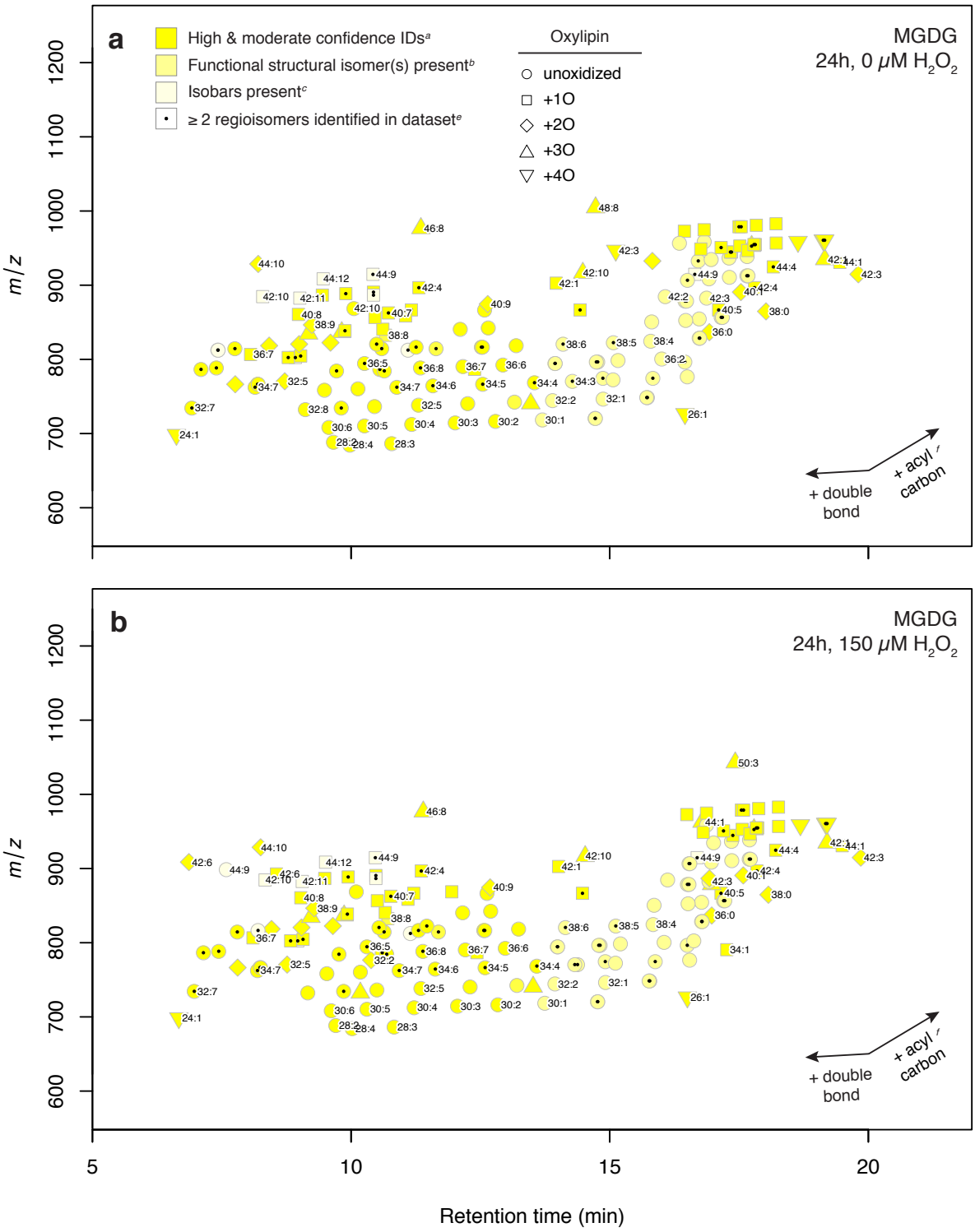
a
High & moderate confidence IDs[a]
Functional structural isomer(s) present[b]
Isobars present[c]
≥ 2 regioisomers identified in dataset[e]
Oxylipin
unoxidized
+1O
+2O
+3O
+4O
MGDG
24h, 0 μM H2O2
+ double bond
+ acyl carbon
b
MGDG
24h, 150 μM H2O2
+ double bond
+ acyl carbon
m/z
Retention time (min)

Figure S6

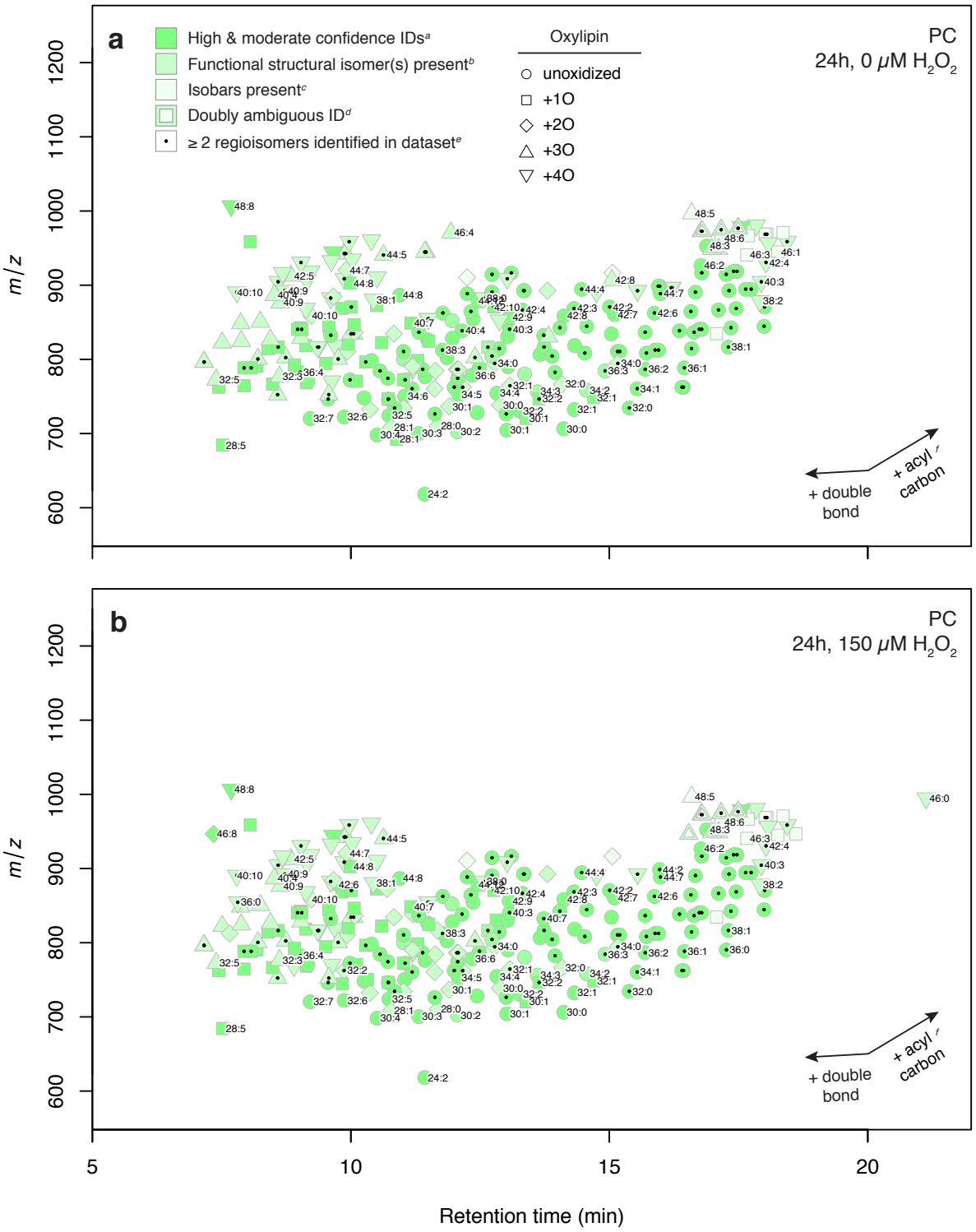
a
High & moderate confidence IDs[a]
Functional structural isomer(s) present[b]
Isobars present[c]
Doubly ambiguous ID[d]
≥ 2 regioisomers identified in dataset[e]
Oxylipin
unoxidized
+1O
+2O
+3O
+4O
PC
24h, 0 μM H2O2
+ double bond
+ acyl carbon
b
PC
24h, 150 μM H2O2
+ double bond
+ acyl carbon
m/z
Retention time (min)

Figure S7

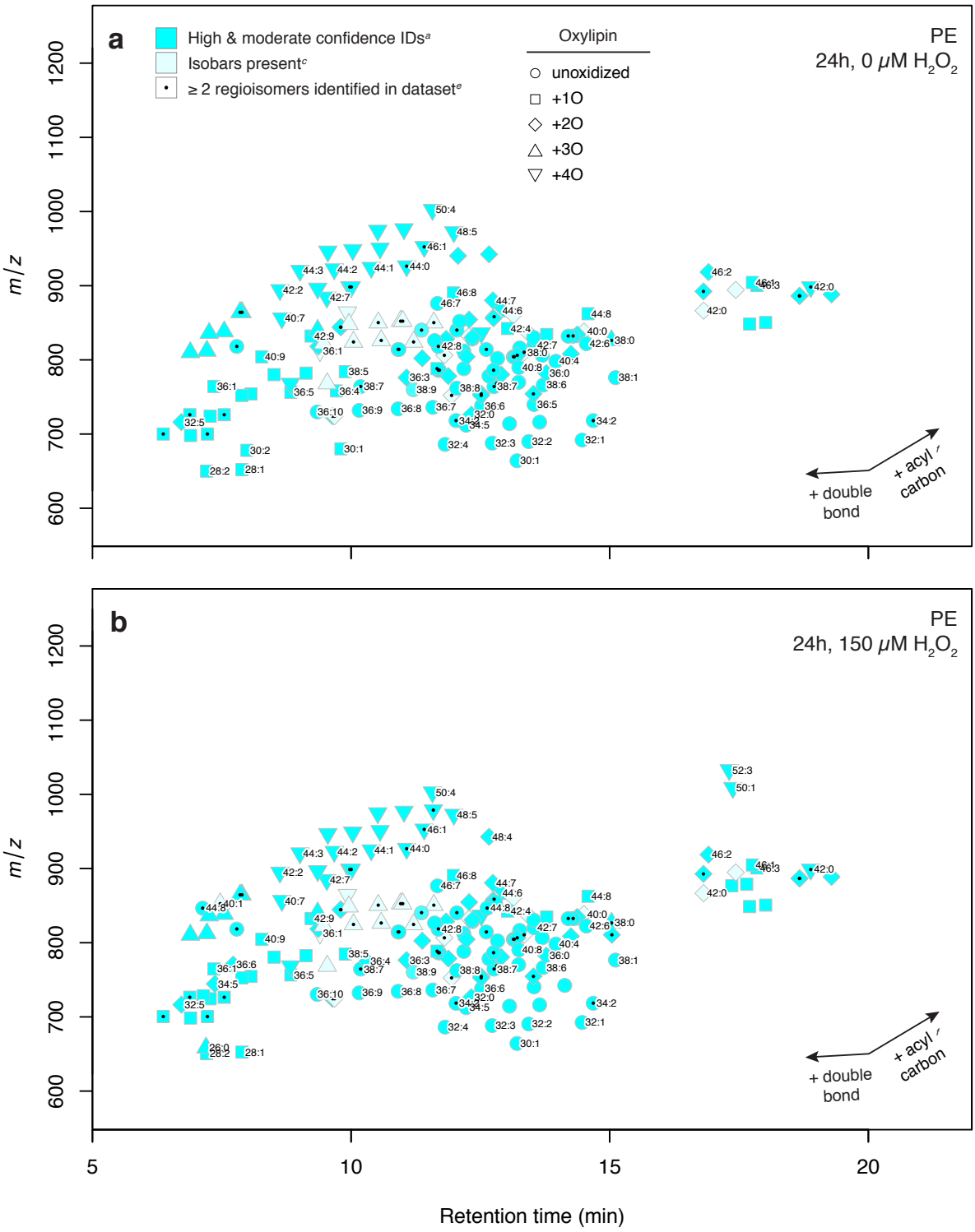
a
High & moderate confidence IDs[a]
Isobars present[c]
≥ 2 regioisomers identified in dataset[e]
Oxylipin
unoxidized
+1O
+2O
+3O
+4O
PE
24h, 0 μM H2O2
+ double bond
+ acyl carbon
b
PE
24h, 150 μM H2O2
m/z
Retention time (min)

Figure S8

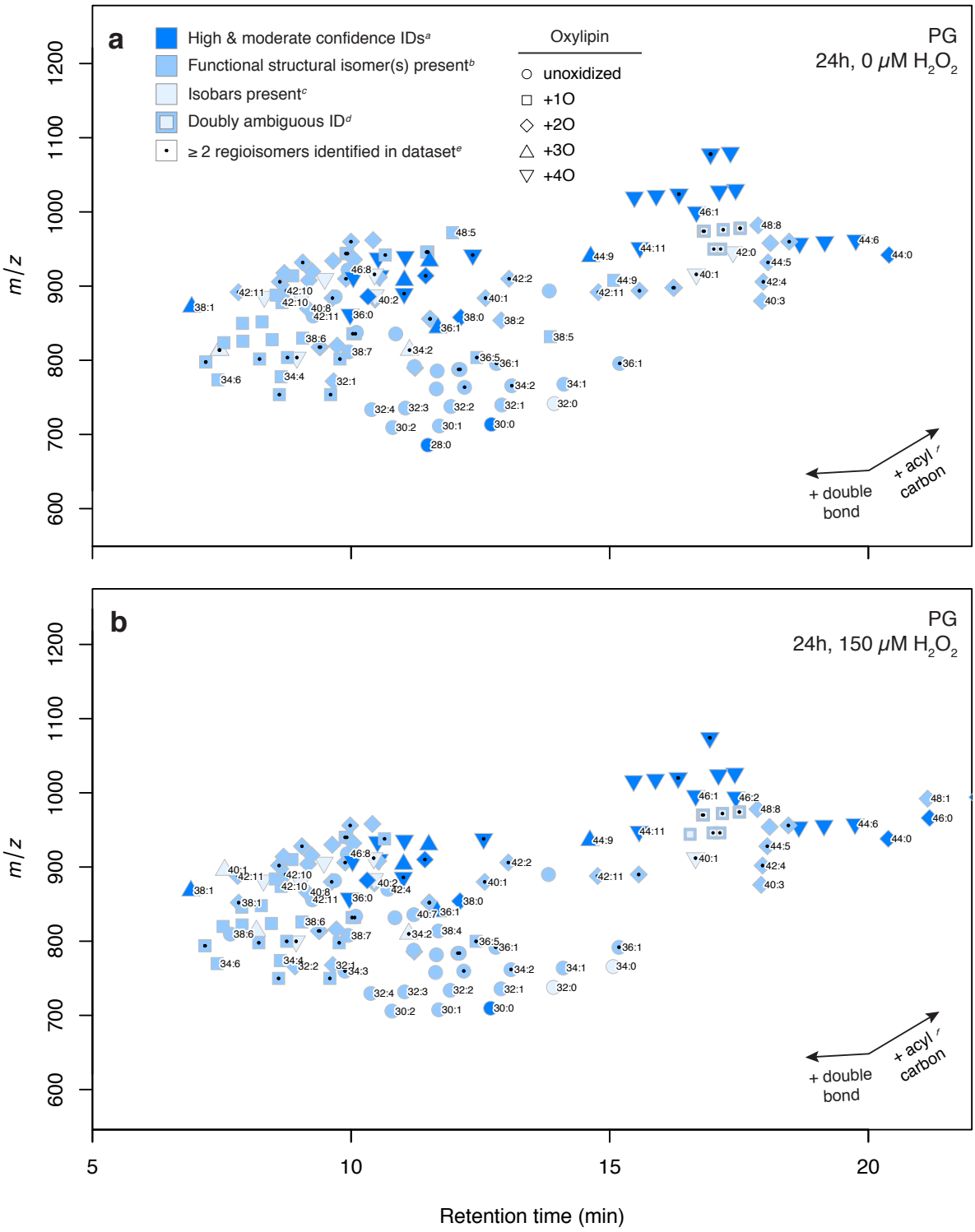
a
High & moderate confidence IDs[a]
Functional structural isomer(s) present[b]
Isobars present[c]
Doubly ambiguous ID[d]
≥ 2 regioisomers identified in dataset[e]
Oxylipin
unoxidized
+1O
+2O
+3O
+4O
PG
24h, 0 μM H2O2
+ double bond
+ acyl carbon
b
PG
24h, 150 μM H2O2
m/z
Retention time (min)

Figure S9

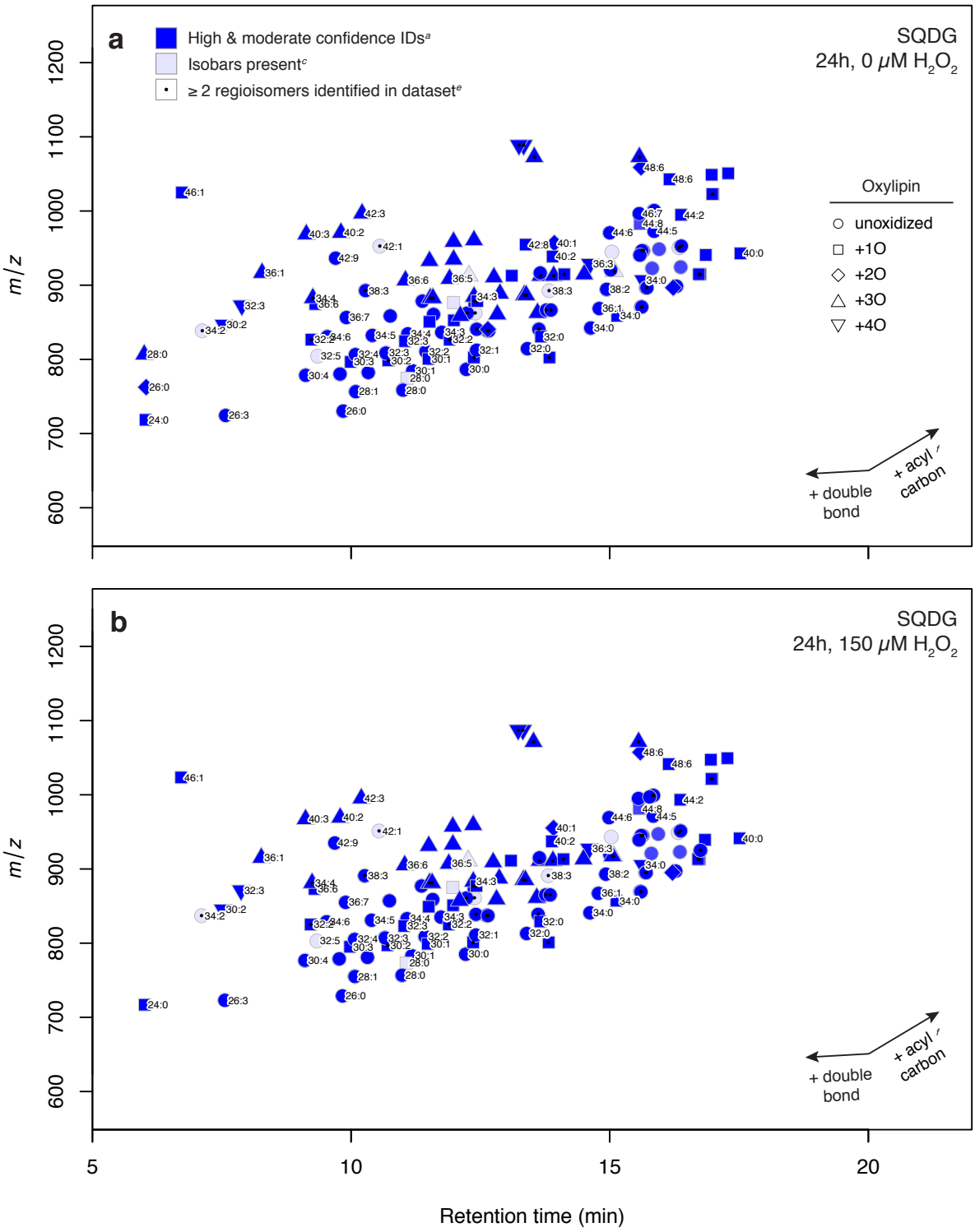
a
High & moderate confidence IDs[a]
Isobars present[c]
≥ 2 regioisomers identified in dataset[e]
SQDG
24h, 0 μM H2O2
Oxylipin
unoxidized
+1O
+2O
+3O
+4O
+ double bond
+ acyl carbon
b
SQDG
24h, 150 μM H2O2
m/z
Retention time (min)

Figure S10

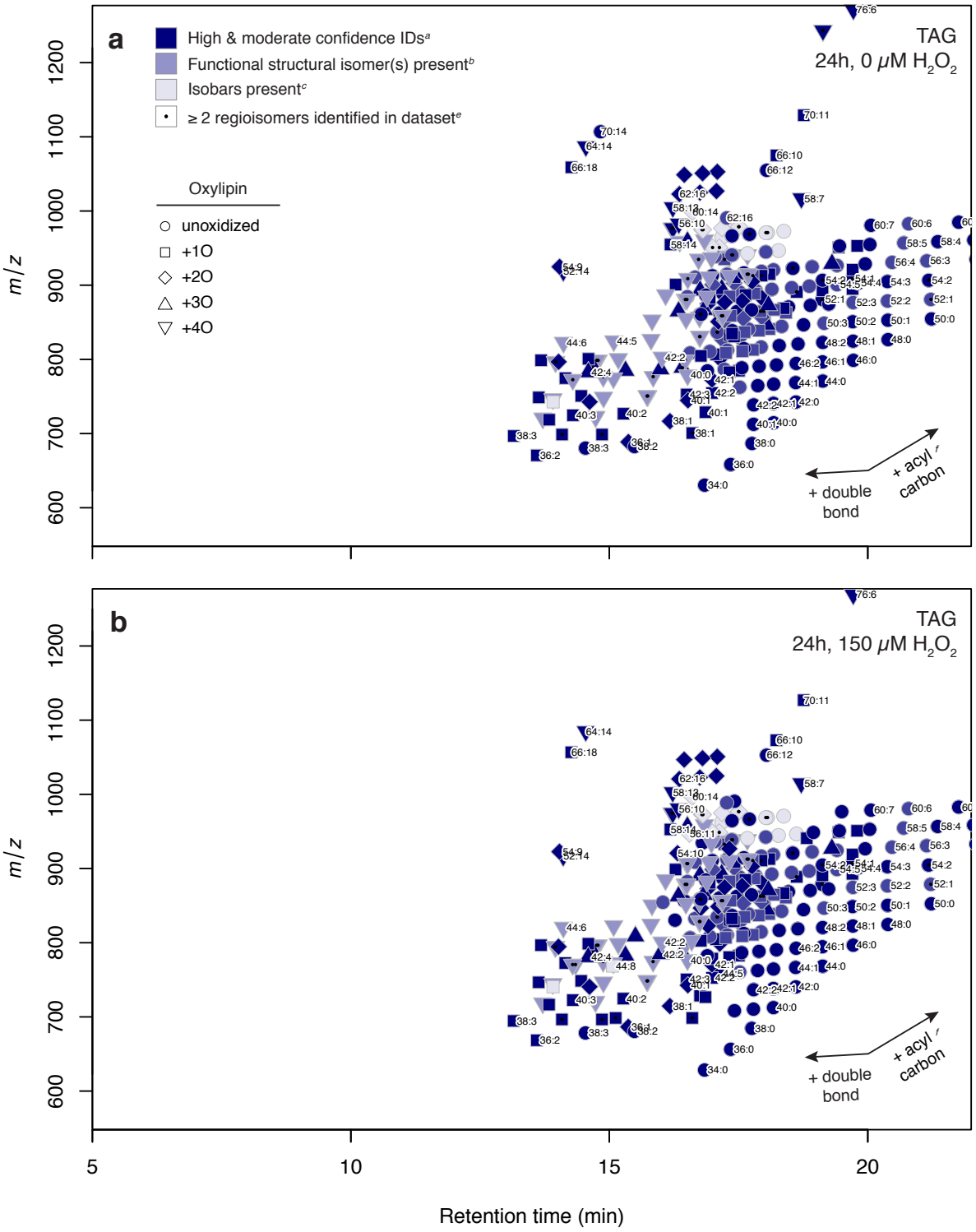
a
High & moderate confidence IDs[a]
Functional structural isomer(s) present[b]
Isobars present[c]
≥ 2 regioisomers identified in dataset[e]
Oxylipin
unoxidized
+1O
+2O
+3O
+4O
TAG
24h, 0 μM H2O2
+ double bond
+ acyl carbon
b
TAG
24h, 150 μM H2O2
+ double bond
+ acyl carbon
m/z
Retention time (min)

Figure S11. An expanded version of the heatmap in Figure 2a, showing remodeling of the *Phaeodactylum tricornutum* lipidome after 24 h. A high-resolution version of the figure is included in a separate .pdf file. Heatmap shows relative abundances across two treatments (0 and 150 μM H_2O_2) of all IPL, ox-IPL, and TAG identified by LOBSTAHS with high confidence. Each row (N = 896) represents a different compound identified from the database. Heatmap shading shows the relative abundance of each compound as a fold difference of the mean peak area observed in that treatment from the mean peak area of the compound observed across all treatments; grey shading indicates the compound was not observed. Dendrogram clustering and group definitions were determined by similarity profile analysis[9] of lipidome components based on changes in relative peak area across treatments; methodological details are described in the Supporting Information text. To facilitate visualization, each group was randomly assigned a different color; group numbers corresponding to those in Table S8 are also indicated. Solid black lines in the dendrogram indicate branching that was statistically significant ($P \leq 0.01$). Table S8 lists the numbers and identities of the components assigned to each group. Data are presented for a single experiment with two technical replicates.

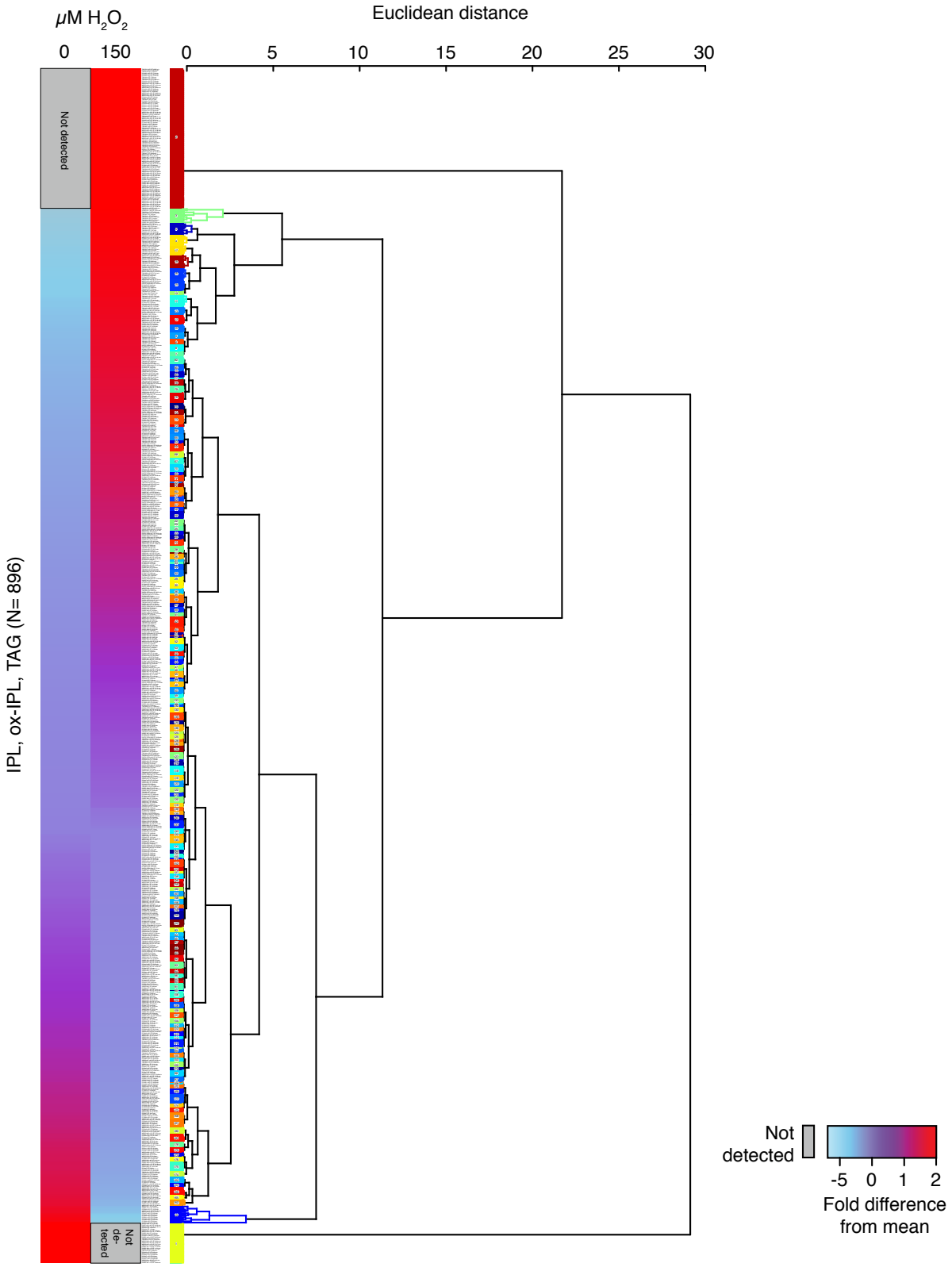
Euclidean distance
0
5
10
15
20
25
30
μM H2O2
0
150
Not detected
Not de-tected
IPL, ox-IPL, TAG (N= 896)
Not detected
-5
0
1
2
Fold difference from mean

Table S1. Database Dimensions and Ranges of Structural Properties Considered for Each Lipid Class

	Ranges of Structural Properties Considered in Creation of Database				Number of Adduct Ions[a]		Total Database Entries[b]	
Compound or Compound Class	Total Acyl Carbon Atoms[c]	Double Bonds[c]	Additional Oxygen Atoms[d]	No. Unique Compounds	Positive Mode	Negative Mode	Positive Mode	Negative Mode
DNP-PE[e]	—	—	—	1	6	5	6	5
FFA	10-26	0-6	0-4	335	—	1	0	335
IP-DAG								
DGCC	20-52	0-12	0-4	1,320	5	7	6,600	9,240
DGDG	20-52	0-12	0-4	1,320	5	7	6,600	9,240
DGTS & A[f]	20-52	0-12	0-4	1,320	5	7	6,600	9,240
MGDG	20-52	0-12	0-4	1,320	5	7	6,600	9,240
PC	20-52	0-12	0-4	1,320	5	7	6,600	9,240
PE	20-52	0-12	0-4	1,320	5	3	6,600	3,960
PG	20-52	0-12	0-4	1,320	6	4	7,920	5,280
SQDG	20-52	0-12	0-4	1,320	6	3	7,920	3,960
Pigments[g]	—	—	—	22	2	6	44	132
PUA	6-12	0-5[h]	0-4[h]	155	1	1	155	155
TAG	30-78	0-18[h]	0-4	2,995	7	—	20,965	0
Total	—	—	—	14,068	—		76,610	60,027

[a] See Table S2. A blank value indicates the compound or compound class was not typically observed or did not readily form this ion in the given mode.

[b] This value reflects all chemically possible combinations of the ranges of properties considered for this compound class.

[c] For FFA, IP-DAG, PUA, and TAG.

[d] For FFA, IP-DAG, and TAG.

[e] Used as internal standard.

[f] The betaine lipids DGTS and DGTA are structural isomers; while they can be resolved chromatographically[15], our current approach requires that they be considered together.

[g] The positive mode database contains entries for adduct ions of 22 different common photosynthetic pigments. See Table S3 for definition of abbreviations. The negative mode database includes only chl *a* since pigments are traditionally identified in positive mode [16].

[h] Not all values of these properties were considered for every possible number of total acyl carbon atoms.

Table S2. Relative Abundances, by Rank, for Adduct Ions of Lipid and Oxylipin Species Reported in the Database

	Pigments[a]	DGCC	DGDG	DGTS & A[b]	DNP-PE[c]	FFA	MGDG	PC	PE	PG	PUA	SQDG	TAG
Positive ion mode													
$[M+H]^+$	1	1	—	1	5	—	—	1	1	3	1	4	—
$[M+K]^+$	†	5	3	5	6	—	4	5	5	6	—	6	6
$[M+NH_4]^+$	†	—	1	—	1	—	1	—	—	1	—	1	1
$[M+Na]+$	2	2	2	2	2	—	2	2	2	2	—	2	2
$[M+2Na-H]^+$	†	4	5	4	3	—	5	4	3	4	—	3	—
$[M+NH_4+ACN]^+$	†	3	4	3	4	—	3	3	4	5	—	5	4
$[M+2Na+Cl]^+$	—	—	—	—	—	—	—	—	—	—	—	—	5
$[M+C_4H_{10}N_3]^+$	—	—	—	—	—	—	—	—	—	—	—	—	7
$[M+C_2H_3Na_2O_2]^+$	—	—	—	—	—	—	—	—	—	—	—	—	3
Negative ion mode													
$[M-H]^-$	—	7	6	7	1	1	7	7	1	1	1	1	—
$[M+Na-2H]^-$	—	—	—	—	3	—	—	—	—	—	—	—	—
$[M+Cl]^-$	3	3	2	3	—	—	2	3	—	—	†	—	—
$[M+K-2H]^-$	—	—	—	—	5	—	—	—	—	4	—	—	—
$[M+HAc-H]^-$	1	1	1	1	—	—	1	1	—	—	†	—	—
$[M+NaAc-H]^-$	—	—	—	—	2	—	—	—	2	2	—	2	—
$[M+Na+Cl-H]^-$	—	—	—	—	4	—	—	—	3	3	—	3	—
$[M+NaAc+Cl]^-$	5	5	5	5	—	—	5	5	—	—	—	—	—
$[M+NaAc+HAc-H]^-$	2	2	2	2	—	—	3	2	—	—	—	—	—
$[M+2NaAc+Cl]^-$	6	6	7	6	—	—	6	6	—	—	—	—	—
$[M+3Ac+2Na]^-$	4	4	4	4	—	—	4	4	—	—	—	—	—

Adduct ion abundance rankings were determined empirically using standards under the HPLC-ESI-MS conditions described in the text. To obtain abundance rankings for ox-IPL, we applied the hierarchy observed for the corresponding unoxidized parent IPL. A blank value indicates the compound or compound class was not typically observed or did not readily form this ion in the given mode. A dagger (†) indicates that the adduct ion can be observed, but not in a relative abundance that was consistent across samples.

[a] The databases contain entries for a range of photosynthetic pigments (see Table S3).

[b] The betaine lipids DGTS and DGTA are structural isomers; while they can be resolved chromatographically[1S], our current approach requires that they be considered together.

[c] Used as internal standard.

Table S3. Pigment Abbreviations Used in LOBSTAHS Databases

Pigment	Abbreviation Used in Databases[a]
19'-butanoyloxyfucoxanthin	19prime_but_fuco
19'-hexanoyloxyfucoxanthin	19prime_hex_fuco
Alloxanthin	Allox
α-carotene	Alpha_carotene
β-carotenes	Beta_carotenes
Chlorophyll *a*	Chl_a
Chlorophyll	Chl_b
Chlorophyll c_2	Chl_c2
Chlorophyll c_3	Chl_c3
Chlorophyllide *a*	Chlide_a
Crocoxanthin	Croco
Diadinochrome or diadinoxanthin	Dd_Ddc
Diatoxanthin	Dt
Echinenone	Echin
Fucoxanthin	Fuco
Lutein	Lut
Neoxanthin or nostoxanthin	Neox_Nos
Peridinin	Peri
Pheophytin *a*	Pheophytin_a
Prasinoxanthin	Pras
Violaxanthin	Viol
Zeaxanthin	Zeax

The default LOBSTAHS databases contain entries for adduct ions of 22 different common photosynthetic pigments

[a] If given, this abbreviation is used in the databases in lieu of the full compound name. Abbreviations follow from Egeland.[16] If no abbreviation is given, the full name of the compound is used in the databases. In some cases (e.g., α-carotene, β-carotene, diadinochrome or diadinoxanthin), the database entries for adduct ions of a given pigment will encompass many possible isomers. For each pigment, the databases contain separate entries for the exact masses of multiple adduct ions; in some cases, the relative abundances of these adduct ions are not listed since they were not determined.

Table S4. Retention Time Window Criteria for Various Compounds and Compound Classes

Lipid Class or Compound[a]	Minimum RT (min.)	Maximum RT (min.)
DGCC	7	20.4
DGDG	5	19
DGTS & DGTA	7	20.6
DNP-PE	14.7	—
FFA	—	—
MGDG	7.1	21.1
PC	6.7	20.7
PE	6.7	20.7
PG	6.7	20.7
19'-hex-fuco	10.2	10.8
Allox	10.8	—
β-carotenes	10.8	—
Chl *a*	15.7	—
Chl *b*	—	—
Chl c_2	5.6	—
Chlide *a*	5.6	15.8
Croco	15.3	—
Dd or Ddc	8.5	—
Dt	—	—
Echin	15.3	—
Fuco	7.7	—
Lut	13.4	—
Neox or Nos	8	—
Peri	—	—
Pheophytin *a*	16.2	—
Pras	8	—
Viol	8	—
Zeax	13.4	—
SQDG	6.5	18.5
TAG	15	22.7

The retention times given in this table are the LOBSTAHS package defaults. RT window data were obtained from authentic standards for representative compounds of each parent lipid class under the chromatographic conditions described in the text. For some compounds or compound classes, minimum or maximum retention times could not be determined. LOBSTAHS users outside of the Van Mooy Lab at WHOI who wish to include screening based on retention time should download a Microsoft Excel spreadsheet included with the package at https://github.com/vanmooylipidomics/LOBSTAHS/ This spreadsheet can be used to generate a table of retention time windows particular to the user's own chromatography; this table can then be imported by specifying a value for rt.windows when calling the function `doLOBscreen()`.

[a] See Table S3 for pigment abbreviations.

Table S5. xcms, CAMERA, and LOBSTAHS Settings Used in Analysis of the *P. tricornutum* Dataset

Parameter	Value
xcms	
xcmsSet()	
method	centWave
profparam[a]	list(step=0.001)
ppm	2.5
min./max. peakwidth[b]	35, 88
fitgauss	TRUE
noise	500
mzdiff[b]	0.002432
verbose.columns	TRUE
snthresh	10
integrate	1
prefilter[b]	3, 19000
mzCenterFun	wMean
group()[c]	
method	density
bw[b]	15
minfrac[b]	0.38
minsamp	2
mzwid[b]	0.001
max	50
retcor()	
method	loess
missing[b]	3
extra[b]	1
smooth	loess
span[b]	0.3
family	gaussian
fillPeaks()	
method	chrom
CAMERA	
annotate()	
quick	FALSE
sample	NA
sigma	6
perfwhm	0.6
cor_eic_th	0.75
graphMethod	hcs
pval	0.05
calcCiS	TRUE
calcIso	TRUE

calcCaS	FALSE
maxcharge	4
maxiso	0.5
minfrac	0.5
psg_list	NULL
rules	NULL
polarity	positive
multiplier	3
max_peaks	100
intval	into
ppm	2.5
mzabs	0.0015
LOBSTAHS	
doLOBscreen()	
polarity	positive
database	NULL[d]
remove.iso	TRUE
rt.restrict	TRUE
rt.windows	NULL[d]
exclude.oddFA	TRUE
match.ppm	2.5

The R script "prepOrbidata.R" can be used to apply the xcms and CAMERA settings presented here in a single sequence. The is not part of the LOBSTAHS R package, but can be downloaded as part of the Van Mooy Lab Lipidomics Toolbox from https://github.com/vanmooylipidomics/LipidomicsToolbox/

[a] Because the mass accuracy of the Orbitrap can surpass the width of the *m/z* windows used to define each peak, a very small value should be used for `profparam`.

[b] Values for these parameters were optimized using the IPO [17] package. Where applicable, we used the values in Table 1 of Patti et al.[18] as initial values for IPO optimization.

[c] The `group()` function was applied to the data twice: Once after `xcmsSet()` and then again after `retcor()`. The parameter values given here were used in both instances.

[d] `doLOBscreen()` applies the LOBSTAHS package defaults when NULL (or no value) is specified for these parameters. The default database is described in Tables S1 and S2, while the default retention time windows are described in Table S4.

Table S6. Evaluation of Method Performance using IPL standards and Alternative Software for Feature Detection and Chromatographic Alignment

Lipid class	Origin of Standard	Moieties Present in Standard[a]	Dominant Positive Mode Adduct Ion	Ion Exact *m/z*	Observed *m/z*[b]	Relative Mass Uncertainty (ppm)[c]	Correct ID from Default Database Using LOBSTAHS?	Confidence in Assignment After Adduct Hierarchy Screening[d]	Structural Isomers or Isobars Present After Screening?
MGDG	Purified from natural sample	34:0	$[M+NH_4]^+$	776.6246	776.6248	0.2	Yes	High confidence	No
		36:0	$[M+NH_4]^+$	804.6559	804.6559	0.02	Yes	High confidence	No
DNP-PE	Synthetic	32:0	$[M+NH_4]^+$	875.5505	875.5507	0.2	Yes	High confidence	No
SQDG	Purified from natural sample	34:3	$[M+NH_4]^+$	834.5396	834.5397	0.2	Yes	High confidence	No
		34:2	$[M+NH_4]^+$	836.5552	836.5554	0.2	Yes	High confidence	No
PG	Synthetic	32:0	$[M+NH_4]^+$	740.5436	740.5438	0.3	Yes	High confidence	No
PE	Synthetic	32:0	$[M+H]^+$	692.5225	692.5227	0.3	Yes	High confidence	No
PC	Synthetic	32:0	$[M+H]^+$	734.5694	734.5695	0.1	Yes	High confidence	No
DGDG	Purified from natural sample	34:2	$[M+NH_4]^+$	934.6461	934.6463	0.1	Yes	High confidence	No
		36:4	$[M+NH_4]^+$	958.6461	958.6463	0.1	Yes	High confidence	No
Mean						0.2			

The results in this table were obtained as in Table 1 in the text, except that MAVEN [19,20] was used instead of xcms for initial peak picking (feature detection) and chromatographic alignment.

[a] Multiple moieties were present in glycolipid standards purified from natural samples; in these cases, only predominant moieties are shown

[b] Mean observed *m/z* ratio in 5 independent samples

[c] $\left|\frac{\text{Measured exact mass} - \text{Calculated exact mass}}{\text{Calculated exact mass}}\right| \times 10^6$

[d] "High confidence" indicates the assignment fully satisfied all adduct hierarchy rules and other screening criteria applied as described in the text.

Table S7. Annotation of Isomers and Isobars in Screened *P. tricornutum* Dataset

	Peaks (Features) for which Isomer/Isobar Type was Identified		Peak Groups in which Isomer/Isobar Type was Identified		Assignments for which Isomer/Isobar Type was Identified		Parent Compounds for which Isomer/Isobar Type Was Identified	
Type of Feature	No.	% Total Peaks	No.	% Total Peak Groups	No.	% Total Assignments	No.	% Total Parent Compounds
Functional structural isomer	5,057	23	375	24	752	37	577	29
Isobar	1,137	5	84	5	195	9	162	8
Any ambiguity[a]	5,401	25	432	27	893	43	699	36
Regioisomer	7,591	35	556	35	750	36	352	18

[a] Elements having either a functional structural isomer, isobar, or both.

Table S8. List of Groups of *P. Tricornutum* Lipidome Components Determined by Similarity Profile Analysis in 0 μm and 150 μm H_2O_2 Treatments at 24 h

Group No.	Abundance of Group Components in 150 μM H_2O_2 Treatment Relative to 0 μM Control[a]	No. Com-ponents	Component Molecules Assigned by Similarity Profile Analysis		
1	Less abundant (downregulated)	30	MGDG 42:4 +1O, RT 11.33 min	TAG 70:14, RT 14.83 min	PG 42:11 +3O, RT 11.01 min
			DGDG 40:1 +1O, RT 17.75 min	DGDG 36:8 +1O, RT 14.1 min	PE 32:5 +1O, RT 6.36 min
			DGDG 36:1 +1O, RT 16.84 min	DGDG 36:8 +1O, RT 11.64 min	DGDG 36:9, RT 14.05 min
			PE 44:5, RT 12.09 min	TAG 70:11 +1O, RT 18.76 min	SQDG 30:2 +4O, RT 7.52 min
			SQDG 36:1 +3O, RT 8.26 min	MGDG 46:5 +1O, RT 17.17 min	PE 42:4, RT 11.6 min
			PE 40:7 +4O, RT 8.65 min	SQDG 32:3 +2O, RT 12.63 min	PE 40:2, RT 12.82 min
			PE 42:9 +1O, RT 9.22 min	MGDG 38:0 +2O, RT 18.04 min	MGDG 38:6, RT 10.51 min
			PE 38:7 +1O, RT 8.5 min	TAG 66:10 +1O, RT 18.23 min	MGDG 48:8 +1O, RT 16.46 min
			PE 36:5 +1O, RT 8.82 min	TAG 58:7 +4O, RT 18.71 min	DGCC 40:0 +4O, RT 16.36 min
			MGDG 30:6, RT 9.59 min	DGDG 44:8 +1O, RT 16.22 min	PE 40:9 +1O, RT 8.26 min
2	More abundant (upregulated)	105	TAG 52:13 +1O, RT 14.54 min	MGDG 40:6 +2O, RT 15.65 min	PE 40:1 +1O, RT 17.28 min
			TAG 56:3 +2O, RT 18.82 min	TAG 44:4 +3O, RT 15.51 min	PE 52:3 +4O, RT 17.3 min
			MGDG 42:7 +1O, RT 16.89 min	PE 34:1, RT 15.6 min	TAG 56:7 +4O, RT 17.23 min
			MGDG 40:3 +2O, RT 16.9 min	DGDG 36:5 +2O, RT 10.55 min	PE 48:8 +1O, RT 8.37 min
			MGDG 34:2 +1O, RT 16.89 min	TAG 56:15, RT 16.23 min	TAG 48:11, RT 15.7 min
			MGDG 36:6 +1O, RT 6.53 min	TAG 52:10 +1O, RT 16.18 min	DGDG 48:8, RT 7.36 min
			TAG 56:13 +1O, RT 15.93 min	TAG 50:8 +2O, RT 16.18 min	PE 42:4 +2O, RT 7.43 min
			TAG 52:10 +2O, RT 15.88 min	TAG 50:9 +1O, RT 16.18 min	MGDG 44:6 +3O, RT 16.6 min
			MGDG 38:4 +2O, RT 15.9 min	TAG 50:11, RT 16.27 min	MGDG 36:1 +2O, RT 16.74 min
			TAG 50:12, RT 15.87 min	TAG 48:10, RT 16.13 min	MGDG 34:0 +2O, RT 16.69 min
			DGDG 42:1 +2O, RT 9.59 min	MGDG 48:7 +3O, RT 15.22 min	SQDG 42:0, RT 16.66 min
			DGDG 38:9 +2O, RT 8.68 min	MGDG 40:7 +2O, RT 15.17 min	PE 46:1 +4O, RT 16.66 min
			DGDG 36:9 +2O, RT 7.95 min	TAG 38:1 +1O, RT 15.12 min	PG 42:0 +2O, RT 16.66 min
			PC 48:8 +2O, RT 8.97 min	TAG 48:12, RT 15.14 min	MGDG 38:5 +1O, RT 16.66 min

			PG 44:1 +4O, RT 8.97 min	TAG 50:7 +2O, RT 16.51 min	TAG 52:14, RT 15.41 min
			DGDG 36:1, RT 8.48 min	MGDG 34:3 +1O, RT 16.52 min	MGDG 40:4 +1O, RT 11.91 min
			DGDG 32:3 +1O, RT 9.64 min	MGDG 40:5 +2O, RT 15.96 min	MGDG 42:7 +3O, RT 17.09 min
			MGDG 32:6 +1O, RT 8.37 min	MGDG 46:5 +1O, RT 16.02 min	PE 44:4 +1O, RT 17.14 min
			MGDG 24:3 +1O, RT 9.53 min	TAG 46:9, RT 16.09 min	PE 42:3 +1O, RT 17.09 min
			MGDG 48:6 +3O, RT 15.73 min	TAG 48:7 +2O, RT 16 min	TAG 54:9 +1O, RT 17.09 min
			MGDG 42:3 +1O, RT 15.74 min	TAG 64:17, RT 17.38 min	TAG 42:4, RT 17.13 min
			TAG 52:11 +1O, RT 15.77 min	PE 48:2 +4O, RT 16.8 min	TAG 42:4, RT 17.09 min
			TAG 50:9 +2O, RT 15.79 min	PC 44:9 +4O, RT 16.8 min	PE 48:2 +1O, RT 17.84 min
			MGDG 36:6 +1O, RT 15.7 min	MGDG 44:9 +3O, RT 16.78 min	PE 46:0 +1O, RT 18.02 min
			DGDG 36:5 +1O, RT 13.18 min	PG 42:2 +4O, RT 16.8 min	PG 46:2 +4O, RT 17.44 min
			PC 32:3 +1O, RT 9.85 min	MGDG 42:4 +3O, RT 16.81 min	PE 44:1 +2O, RT 20.39 min
			MGDG 42:8 +2O, RT 15.31 min	MGDG 36:0 +3O, RT 16.77 min	TAG 64:16, RT 17.53 min
			TAG 36:1 +1O, RT 13.83 min	TAG 44:6, RT 16.77 min	MGDG 44:4 +1O, RT 15.86 min
			MGDG 36:9 +4O, RT 7.02 min	TAG 56:11 +1O, RT 16.95 min	SQDG 30:2 +1O, RT 8.39 min
			DGDG 46:7 +4O, RT 14.66 min	MGDG 40:6 +3O, RT 16.95 min	MGDG 38:4 +3O, RT 15.76 min
			MGDG 36:8 +1O, RT 11.35 min	MGDG 38:1 +3O, RT 16.94 min	MGDG 32:2 +2O, RT 10.36 min
			DGDG 36:7 +1O, RT 11.19 min	PE 44:2 +1O, RT 16.99 min	MGDG 40:7 +1O, RT 16.47 min
			MGDG 24:3, RT 11.78 min	DGDG 44:2 +1O, RT 17.32 min	PE 40:2 +1O, RT 16.95 min
			MGDG 40:4 +3O, RT 16.39 min	PE 50:1 +4O, RT 17.37 min	SQDG 38:4 +4O, RT 17.47 min
			TAG 44:7, RT 16.43 min	PE 44:1 +1O, RT 17.35 min	TAG 52:11 +2O, RT 15.3 min
3	More abundant	11	TAG 54:12, RT 16.87 min	TAG 54:8 +1O, RT 17.43 min	TAG 56:13, RT 16.99 min
			SQDG 40:1 +2O, RT 13.91 min	TAG 52:10, RT 17.14 min	TAG 52:8 +1O, RT 16.94 min
			DGDG 32:2 +2O, RT 9.65 min	TAG 52:5 +2O, RT 17.76 min	SQDG 36:6 +1O, RT 9.29 min
			TAG 46:7, RT 16.9 min	TAG 52:11, RT 16.78 min	
4	More abundant	8	TAG 42:2 +3O, RT 15.99 min	TAG 50:6 +2O, RT 16.91 min	TAG 50:5 +2O, RT 17.23 min
			SQDG 32:2 +1O, RT 9.22 min	TAG 58:13, RT 17.38 min	MGDG 42:1 +1O, RT 13.98 min
			PE 46:1 +1O, RT 17.75 min	MGDG 36:0 +2O, RT 16.94 min	
5	More abundant	9	TAG 60:14, RT 17.37 min	TAG 42:4 +3O, RT 14.59 min	SQDG 40:2 +1O, RT 13.88 min

			MGDG 40:5 +1O, RT 17.12 min	TAG 54:11, RT 17.2 min	PE 46:3 +1O, RT 17.83 min
			PG 38:1 +3O, RT 6.9 min	TAG 52:9, RT 17.47 min	MGDG 46:8 +1O, RT 17.35 min
6	More abundant	4	TAG 48:4 +1O, RT 17.38 min	TAG 50:1, RT 20.39 min	TAG 52:4, RT 19.25 min
			TAG 46:4, RT 17.9 min		
7	More abundant	4	SQDG 40:7 +3O, RT 12.36 min	TAG 52:5, RT 18.89 min	MGDG 46:7 +1O, RT 17.68 min
			MGDG 32:5 +2O, RT 8.73 min		
8	More abundant	5	TAG 50:0, RT 21.23 min	TAG 44:3, RT 17.87 min	PC 40:1, RT 14.58 min
			DGTS_DGTA 40:1, RT 18.08 min	PC 36:2, RT 15.71 min	
9	More abundant	5	MGDG 44:1 +1O, RT 19.46 min	PG 44:0 +2O, RT 20.39 min	PE 42:10, RT 12.6 min
			TAG 44:6 +1O, RT 14.15 min	TAG 54:2, RT 19.13 min	
10	More abundant	6	TAG 44:0, RT 19.13 min	DGDG 32:5, RT 10.56 min	TAG 56:8, RT 18.55 min
			PE 40:2 +2O, RT 14.36 min	MGDG 36:9 +2O, RT 8.43 min	TAG 42:1, RT 18.18 min
11	More abundant	9	TAG 44:2 +1O, RT 17.32 min	PE 38:1 +2O, RT 14.24 min	PC 44:4, RT 17.65 min
			TAG 52:6 +1O, RT 17.63 min	PC 46:8 +4O, RT 17.57 min	PE 42:5 +2O, RT 12.74 min
			TAG 52:8, RT 17.75 min	DGDG 48:4 +1O, RT 17.42 min	TAG 48:5 +1O, RT 17.33 min
12	More abundant	7	MGDG 44:4 +1O, RT 18.18 min	TAG 52:1, RT 19.12 min	MGDG 42:4 +1O, RT 17.81 min
			PE 40:4 +2O, RT 12.34 min	MGDG 36:9 +1O, RT 8.8 min	TAG 54:3 +1O, RT 19.71 min
			DGDG 32:5, RT 10.46 min		
13	More abundant	6	PC 44:4, RT 17.76 min	SQDG 34:4 +3O, RT 9.25 min	TAG 42:3 +3O, RT 15.31 min
			TAG 56:11, RT 17.6 min	DGTS_DGTA 38:7, RT 14.32 min	TAG 42:1 +3O, RT 16.41 min
14	More abundant	3	TAG 48:6, RT 17.6 min	PC 48:8 +1O, RT 8.07 min	TAG 58:1, RT 24.67 min
15	More abundant	9	TAG 46:4 +1O, RT 17.07 min	MGDG 42:3 +4O, RT 15.13 min	DGDG 36:7 +2O, RT 8.8 min
			DGTS_DGTA 30:0, RT 14.5 min	PC 34:0, RT 16.42 min	TAG 54:1, RT 19.69 min
			MGDG 44:6 +3O, RT 17.76 min	PC 32:0, RT 15.4 min	TAG 42:2, RT 17.79 min
16	More abundant	8	PC 38:5, RT 15.73 min	TAG 46:0, RT 19.72 min	TAG 60:13, RT 17.71 min
			TAG 46:5, RT 17.56 min	PC 34:0, RT 16.45 min	MGDG 38:9 +2O, RT 9.26 min
			DGTS_DGTA 44:12, RT 6.67 min	TAG 48:6 +1O, RT 17.41 min	
17	More abundant	7	PC 42:11 +1O, RT 9.84 min	TAG 54:7 +1O, RT 17.95 min	TAG 48:4 +2O, RT 17.11 min
			TAG 50:8, RT 17.38 min	TAG 60:5, RT 21.76 min	TAG 46:5 +1O, RT 16.77 min

			PC 32:2 +1O, RT 10.74 min		
18	More abundant	10	PC 36:9 +1O, RT 8.09 min	TAG 50:2 +2O, RT 17.95 min	TAG 50:4 +2O, RT 17.57 min
			TAG 44:1 +2O, RT 17.14 min	TAG 42:5 +1O, RT 13.64 min	TAG 48:0, RT 20.39 min
			DGDG 48:3 +1O, RT 17.79 min	MGDG 36:7 +2O, RT 9.62 min	DGTS_DGTA 42:2, RT 17.94 min
			PE 42:1 +1O, RT 17.69 min		
19	Less abundant	13	PC 34:7 +1O, RT 7.95 min	PG 36:0 +4O, RT 9.97 min	DGDG 44:11, RT 13.57 min
			PC 36:8 +1O, RT 8.2 min	MGDG 34:7, RT 8.16 min	PE 38:3 +1O, RT 11.65 min
			PE 30:1 +1O, RT 9.79 min	MGDG 40:10, RT 12.13 min	PE 42:7 +4O, RT 9.52 min
			PE 42:0 +4O, RT 9.99 min	MGDG 44:10 +2O, RT 8.22 min	PE 36:6 +1O, RT 8.05 min
			PC 34:6 +1O, RT 8.5 min		
20	More abundant	3	DGTS_DGTA 50:3, RT 19.7 min	DGDG 34:5, RT 11.83 min	DGTS_DGTA 42:0, RT 18.89 min
21	More abundant	5	PC 40:1, RT 18.01 min	SQDG 32:0 +1O, RT 13.66 min	DGDG 40:1, RT 17.42 min
			PE 48:3 +4O, RT 11.01 min	MGDG 36:8 +2O, RT 9.01 min	
22	More abundant	3	PG 38:0 +2O, RT 12.11 min	TAG 58:2, RT 23.2 min	PC 44:5, RT 13.37 min
23	More abundant	3	MGDG 34:5, RT 8.22 min	DGTS_DGTA 40:7, RT 14.31 min	DGTS_DGTA 42:4, RT 17.22 min
24	More abundant	2	TAG 54:2, RT 21.18 min	TAG 54:2, RT 21.18 min	TAG 54:2, RT 21.18 min
			TAG 54:2, RT 21.18 min	TAG 54:4, RT 19.81 min	
25	More abundant	4	PC 36:1, RT 16.47 min	DGTS_DGTA 36:1, RT 16.82 min	DGTS_DGTA 44:5, RT 17.43 min
			MGDG 26:1 +4O, RT 16.47 min		
26	More abundant	4	SQDG 34:2 +3O, RT 13.33 min	DGTS_DGTA 42:7, RT 15.37 min	SQDG 34:2 +3O, RT 13.37 min
			MGDG 42:7 +1O, RT 10.45 min		
27	More abundant	1	SQDG 46:1 +1O, RT 6.71 min	SQDG 46:1 +1O, RT 6.71 min	SQDG 46:1 +1O, RT 6.71 min
			SQDG 46:1 +1O, RT 6.71 min		
28	More abundant	5	PE 40:8, RT 13.23 min	TAG 56:2, RT 22.1 min	PE 34:0 +2O, RT 12.51 min
			PC 42:3, RT 14.33 min	PE 38:3 +4O, RT 12.51 min	
29	More abundant	3	PC 30:4, RT 10.52 min	DGTS_DGTA 40:2, RT 17.42 min	DGDG 34:5, RT 11.81 min
30	More abundant	6	DGTS_DGTA 38:3, RT 16.08 min	TAG 46:7 +1O, RT 14.6 min	PC 38:6, RT 13.67 min
			MGDG 36:8 +1O, RT 9.04 min	PC 42:10, RT 12.38 min	PC 40:7, RT 13.75 min
31	NS[b]	2	PC 32:6, RT 9.89 min	PC 32:6, RT 9.89 min	PC 32:6, RT 9.89 min

			PC 32:6, RT 9.89 min	TAG 38:2 +1O, RT 14.09 min	
32	More abundant	5	TAG 74:6 +4O, RT 19.13 min	SQDG 36:4 +1O, RT 12.42 min	PC 38:7, RT 13.91 min
			PC 36:7 +1O, RT 8.92 min	TAG 38:2, RT 15.49 min	
33	More abundant	2	PC 36:4, RT 13.96 min	PC 36:4, RT 13.96 min	PC 36:4, RT 13.96 min
			PC 36:4, RT 13.96 min	PC 40:5, RT 15.71 min	
34	More abundant	4	DGDG 32:4, RT 11.28 min	TAG 40:3 +1O, RT 14.3 min	SQDG 36:4 +1O, RT 12.37 min
			PC 38:3, RT 15.9 min		
35	More abundant	1	TAG 50:4 +3O, RT 17.18 min	TAG 50:4 +3O, RT 17.18 min	TAG 50:4 +3O, RT 17.18 min
			TAG 50:4 +3O, RT 17.18 min		
36	More abundant	4	PE 38:4, RT 13.23 min	TAG 58:3, RT 22.05 min	DGTS_DGTA 44:1, RT 18.94 min
			DGDG 34:1, RT 15.27 min		
37	More abundant	3	DGTS_DGTA 34:3, RT 14.02 min	DGDG 40:10, RT 11.38 min	SQDG 36:3 +3O, RT 13.9 min
38	More abundant	6	TAG 40:2 +2O, RT 14.62 min	MGDG 36:10, RT 10.66 min	PC 36:9, RT 10 min
			DGDG 34:4, RT 12.74 min	DGTS_DGTA 34:6, RT 12.94 min	DGTS_DGTA 40:5, RT 16 min
39	More abundant	4	DGDG 34:6, RT 10.8 min	PE 42:2, RT 13.52 min	DGDG 34:2, RT 14.3 min
			PE 36:1 +2O, RT 12.89 min		
40	More abundant	4	PC 34:4 +1O, RT 10.12 min	DGDG 34:3, RT 13.33 min	DGDG 38:9, RT 10.92 min
			PC 42:4, RT 13.33 min		
41	More abundant	3	TAG 62:14 +2O, RT 17.07 min	DGTS_DGTA 34:5, RT 12.5 min	PE 40:1, RT 13.14 min
42	More abundant	8	TAG 54:3, RT 20.38 min	TAG 40:0, RT 18.18 min	MGDG 44:11 +4O, RT 18.65 min
			SQDG 36:6, RT 10.74 min	DGDG 44:3 +3O, RT 16.66 min	DGDG 36:9, RT 9.88 min
			PC 34:1, RT 11.2 min	PC 38:1, RT 17.32 min	
43	NS	2	PC 46:6, RT 17.48 min	PC 46:6, RT 17.48 min	PC 46:6, RT 17.48 min
			PC 46:6, RT 17.48 min	DGTS_DGTA 34:8, RT 9.86 min	
44	More abundant	1	PE 34:4, RT 13.05 min	PE 34:4, RT 13.05 min	PE 34:4, RT 13.05 min
			PE 34:4, RT 13.05 min		
45	More abundant	5	DGDG 34:7, RT 10.15 min	SQDG 48:3 +1O, RT 16.95 min	SQDG 34:3, RT 11.74 min
			MGDG 30:4, RT 11.19 min	MGDG 44:10 +4O, RT 19.14 min	
46	More abundant	2	SQDG 34:3 +1O, RT 11.97 min	SQDG 34:3 +1O, RT 11.97 min	SQDG 34:3 +1O, RT 11.97 min

			SQDG 34:3 +1O, RT 11.97 min	MGDG 46:8 +3O, RT 11.36 min	
47	More abundant	3	DGDG 32:1, RT 14.1 min	PC 40:9, RT 11.98 min	TAG 52:14 +4O, RT 14.11 min
48	More abundant	4	DGTS_DGTA 40:11, RT 11.22 min	SQDG 48:2 +1O, RT 17.28 min	PE 46:8 +1O, RT 11.97 min
			SQDG 34:4, RT 11.08 min		
49	More abundant	3	PC 32:5, RT 10.75 min	DGDG 42:5 +3O, RT 15.46 min	TAG 38:0, RT 17.76 min
50	More abundant	5	PC 42:9, RT 13.08 min	SQDG 34:0 +1O, RT 15.13 min	MGDG 42:1 +3O, RT 19.17 min
			DGDG 46:7 +3O, RT 15.75 min	DGDG 38:8, RT 11.59 min	
51	More abundant	4	DGTS_DGTA 40:6, RT 15.29 min	DGDG 30:0, RT 13.87 min	DGDG 30:2, RT 11.85 min
			DGDG 34:3, RT 13.33 min		
52	More abundant	5	SQDG 38:1, RT 15.7 min	DGDG 40:3, RT 16.28 min	PC 44:5, RT 17.33 min
			MGDG 42:3 +2O, RT 19.82 min	PE 30:2 +1O, RT 7.98 min	
53	More abundant	5	PE 38:2 +2O, RT 13.2 min	SQDG 36:5, RT 11.58 min	PC 36:1, RT 12.5 min
			SQDG 36:4, RT 12.23 min	PC 44:12, RT 12.48 min	
54	More abundant	4	DGTS_DGTA 42:5, RT 16.76 min	DGDG 30:1, RT 12.85 min	SQDG 38:6 +3O, RT 11.97 min
			PC 38:7 +1O, RT 9.97 min		
55	More abundant	2	PE 42:11 +2O, RT 9.78 min	PE 42:11 +2O, RT 9.78 min	PE 42:11 +2O, RT 9.78 min
			PE 42:11 +2O, RT 9.78 min	DGDG 30:2 +4O, RT 12.95 min	
56	More abundant	4	PC 40:6, RT 15.06 min	PC 42:9 +1O, RT 10.51 min	PE 46:1 +4O, RT 11.4 min
			SQDG 30:3 +1O, RT 9.98 min		
57	More abundant	4	DGTS_DGTA 46:6, RT 17.57 min	DGDG 28:0 +2O, RT 12.5 min	DGDG 42:1 +3O, RT 16.94 min
			TAG 50:1 +1O, RT 18.37 min		
58	More abundant	3	DGTS_DGTA 34:0, RT 17 min	PE 42:0 +1O, RT 18 min	DGTS_DGTA 40:4, RT 16.56 min
59	More abundant	6	PG 42:3 +4O, RT 11.03 min	PC 40:8 +1O, RT 10.08 min	PE 50:4 +4O, RT 11.56 min
			PC 32:2 +1O, RT 13.66 min	TAG 44:3 +2O, RT 14.02 min	TAG 52:0, RT 22.22 min
60	More abundant	6	PC 34:1, RT 15.55 min	DGTS_DGTA 42:3, RT 17.56 min	SQDG 46:2 +1O, RT 16.97 min
			PC 32:7, RT 9.23 min	DGDG 36:7 +1O, RT 8.9 min	DGTS_DGTA 44:0, RT 19.5 min
61	More abundant	4	PC 32:0, RT 10.86 min	TAG 48:3, RT 18.65 min	TAG 74:6 +4O, RT 19.13 min
			PC 42:10 +1O, RT 12.78 min		
62	More abundant	5	PC 36:0, RT 13.05 min	MGDG 34:5, RT 8.21 min	TAG 52:3 +1O, RT 19.12 min

			DGTS_DGTA 46:6, RT 17.57 min	PC 38:4, RT 15.17 min	
63	More abundant	2	TAG 52:6, RT 18.47 min	TAG 52:6, RT 18.47 min	TAG 52:6, RT 18.47 min
			TAG 52:6, RT 18.47 min	TAG 48:4, RT 18.29 min	
64	More abundant	6	PE 38:6, RT 13.7 min	TAG 46:2, RT 18.62 min	PC 46:7, RT 13.12 min
			TAG 42:2 +1O, RT 16.99 min	DGTS_DGTA 30:5, RT 7.22 min	DGTS_DGTA 44:1, RT 18.96 min
65	More abundant	5	PC 42:2, RT 18.02 min	MGDG 32:7 +2O, RT 7.77 min	TAG 50:5 +3O, RT 16.76 min
			TAG 56:0, RT 24.78 min	TAG 46:1, RT 19.12 min	
66	More abundant	5	PE 40:9, RT 12.17 min	TAG 54:0, RT 23.41 min	TAG 58:4, RT 21.36 min
			TAG 52:7, RT 18.08 min	PC 44:5, RT 13.36 min	
67	More abundant	5	PC 44:6, RT 12.74 min	MGDG 44:8 +2O, RT 15.84 min	TAG 54:0, RT 23.35 min
			TAG 52:4 +1O, RT 18.63 min	DGTS_DGTA 36:5, RT 13.7 min	
68	More abundant	5	TAG 46:3, RT 18.24 min	TAG 58:7, RT 19.45 min	PC 38:1, RT 13.75 min
			PE 48:4 +2O, RT 12.66 min	DGTS_DGTA 38:1, RT 17.46 min	
69	More abundant	2	DGTS_DGTA 34:4, RT 13.05 min	DGTS_DGTA 34:4, RT 13.05 min	DGTS_DGTA 34:4, RT 13.05 min
			DGTS_DGTA 34:4, RT 13.05 min	PC 36:10, RT 9.18 min	
70	More abundant	6	PC 42:5, RT 12.34 min	PC 38:4, RT 15.22 min	TAG 48:2, RT 19.13 min
			DGTS_DGTA 50:3, RT 19.72 min	TAG 52:4 +1O, RT 18.62 min	PE 42:1, RT 14.28 min
71	More abundant	5	PC 38:3, RT 15.97 min	TAG 42:4 +1O, RT 14.46 min	PC 36:4 +1O, RT 11.31 min
			SQDG 46:2 +1O, RT 16.98 min	PC 38:5, RT 14.54 min	
72	More abundant	2	PC 40:2, RT 14.06 min	PC 40:2, RT 14.06 min	PC 40:2, RT 14.06 min
			PC 40:2, RT 14.06 min	TAG 50:2, RT 19.71 min	
73	More abundant	7	DGDG 32:6, RT 9.74 min	PC 42:2, RT 15.02 min	TAG 60:7, RT 20.06 min
			PE 36:0 +2O, RT 13.76 min	TAG 40:1, RT 17.79 min	TAG 56:5, RT 19.95 min
			PC 38:5 +1O, RT 11.52 min		
74	More abundant	4	DGTS_DGTA 38:4, RT 15.44 min	TAG 42:0, RT 18.61 min	TAG 50:4, RT 18.76 min
			DGTS_DGTA 34:1, RT 15.78 min		
75	More abundant	5	DGTS_DGTA 34:2, RT 14.88 min	PC 36:9 +1O, RT 7.95 min	PG 42:0 +2O, RT 11.43 min
			DGTS_DGTA 34:1, RT 16.57 min	TAG 44:1 +1O, RT 17.51 min	
76	More abundant	8	PC 38:10 +1O, RT 8.41 min	PC 38:0, RT 14.34 min	TAG 58:14 +1O, RT 16.18 min

			TAG 48:1 +3O, RT 18.08 min	TAG 40:2 +1O, RT 15.27 min	PE 36:9, RT 10.15 min
			DGTS_DGTA 40:1, RT 18.04 min	TAG 48:1, RT 19.72 min	
77	More abundant	1	TAG 50:6, RT 18.01 min	TAG 50:6, RT 18.01 min	TAG 50:6, RT 18.01 min
			TAG 50:6, RT 18.01 min		
78	More abundant	5	PC 40:11 +1O, RT 9.06 min	TAG 76:6 +4O, RT 19.72 min	TAG 58:6, RT 20.04 min
			PE 48:5 +2O, RT 12.06 min	DGTS_DGTA 36:4, RT 14.34 min	
79	More abundant	5	TAG 54:1, RT 22.21 min	TAG 54:6 +1O, RT 18.1 min	SQDG 36:3 +3O, RT 13.65 min
			SQDG 36:2 +3O, RT 14.49 min	MGDG 40:1 +2O, RT 17.55 min	
80	More abundant	5	DGDG 30:3, RT 11.24 min	TAG 52:2 +1O, RT 19.7 min	PC 32:1 +1O, RT 14.72 min
			PC 40:11 +1O, RT 8.99 min	TAG 44:1, RT 18.61 min	
81	More abundant	5	DGTS_DGTA 42:10, RT 12.75 min	PC 30:0, RT 14.13 min	TAG 56:8, RT 18.55 min
			PE 34:2, RT 14.67 min	TAG 42:3 +1O, RT 16.5 min	
82	More abundant	6	TAG 44:2, RT 18.18 min	TAG 46:0 +3O, RT 18.05 min	MGDG 40:5 +1O, RT 14.44 min
			PE 40:0, RT 13.69 min	DGTS_DGTA 38:5, RT 14.7 min	PE 42:1, RT 14.19 min
83	Less abundant	4	MGDG 38:9, RT 10.61 min	PE 48:5 +4O, RT 11.98 min	SQDG 32:4, RT 10.07 min
			PE 42:9 +3O, RT 7.84 min		
84	Less abundant	3	TAG 36:1 +2O, RT 15.37 min	TAG 64:15 +2O, RT 17.09 min	PE 42:9 +3O, RT 7.88 min
85	Less abundant	3	PE 40:10, RT 11.69 min	DGTS_DGTA 36:7, RT 11.79 min	PC 36:8, RT 10.73 min
86	Less abundant	3	MGDG 40:9, RT 12.67 min	PC 34:8, RT 9.58 min	PG 40:2 +4O, RT 10.54 min
87	Less abundant	3	TAG 62:15 +2O, RT 16.75 min	TAG 62:16 +2O, RT 16.36 min	SQDG 30:2 +1O, RT 10.7 min
88	Less abundant	5	PC 42:7, RT 15.12 min	TAG 42:1 +3O, RT 14.7 min	DGTS_DGTA 44:7, RT 16.26 min
			MGDG 28:2, RT 9.67 min	PE 40:10, RT 11.68 min	
89	Less abundant	1	SQDG 36:3 +2O, RT 16.21 min	SQDG 36:3 +2O, RT 16.21 min	SQDG 36:3 +2O, RT 16.21 min
			SQDG 36:3 +2O, RT 16.21 min		
90	Less abundant	2	PG 30:0, RT 12.7 min	PG 30:0, RT 12.7 min	PG 30:0, RT 12.7 min
			PG 30:0, RT 12.7 min	PE 44:11, RT 12.03 min	
91	Less abundant	5	DGDG 28:0, RT 5.83 min	PG 38:0 +4O, RT 11.01 min	SQDG 26:0, RT 9.83 min
			PC 38:4, RT 11.04 min	SQDG 32:1 +3O, RT 12.81 min	
92	Less abundant	5	DGDG 32:0 +2O, RT 5.71 min	SQDG 48:6 +2O, RT 15.59 min	PE 38:4 +2O, RT 11.36 min

			SQDG 42:1, RT 16.37 min	SQDG 36:2, RT 13.85 min	
93	Less abundant	5	DGTS_DGTA 44:7, RT 16.21 min	SQDG 48:7 +3O, RT 15.56 min	PE 44:3 +2O, RT 19.28 min
			SQDG 34:0 +4O, RT 15.63 min	PC 34:5, RT 12.1 min	
94	Less abundant	4	DGDG 30:0 +1O, RT 5.78 min	PE 42:8, RT 7.78 min	SQDG 36:0, RT 15.59 min
			PE 28:1 +1O, RT 7.88 min		
95	Less abundant	2	TAG 56:1 +1O, RT 19.79 min	TAG 56:1 +1O, RT 19.79 min	TAG 56:1 +1O, RT 19.79 min
			TAG 56:1 +1O, RT 19.79 min	PC 40:3, RT 16.76 min	
96	Less abundant	3	MGDG 42:9 +1O, RT 9.46 min	MGDG 42:11, RT 12.6 min	PC 36:8, RT 12.08 min
97	Less abundant	4	SQDG 38:10, RT 11.36 min	PG 36:1 +3O, RT 11.66 min	DGDG 50:3 +3O, RT 17.56 min
			PE 36:7 +1O, RT 7.88 min		
98	Less abundant	5	TAG 40:6 +1O, RT 13.84 min	PC 34:7, RT 10.27 min	SQDG 48:7 +4O, RT 13.32 min
			PE 34:2, RT 12.02 min	MGDG 40:10 +1O, RT 10.48 min	
99	Less abundant	3	PE 32:4, RT 11.81 min	PE 42:6, RT 14.54 min	SQDG 32:0 +3O, RT 13.59 min
100	Less abundant	4	MGDG 40:8 +1O, RT 9 min	TAG 66:12, RT 18.04 min	MGDG 36:8, RT 11.36 min
			DGDG 44:9 +1O, RT 15.8 min		
101	Less abundant	2	PC 34:5 +1O, RT 9.15 min	PC 34:5 +1O, RT 9.15 min	PC 34:5 +1O, RT 9.15 min
			PC 34:5 +1O, RT 9.15 min	MGDG 36:6, RT 12.95 min	
102	Less abundant	4	MGDG 30:3, RT 12.03 min	PE 46:7, RT 11.66 min	TAG 38:2 +1O, RT 14.86 min
			SQDG 34:1, RT 12.41 min		
103	Less abundant	3	TAG 36:2 +1O, RT 13.6 min	PG 48:3 +4O, RT 16.32 min	SQDG 48:7 +4O, RT 13.23 min
104	Less abundant	4	PE 32:3, RT 12.72 min	MGDG 32:4, RT 12.27 min	PC 46:7, RT 16.8 min
			SQDG 28:1, RT 10.08 min		
105	Less abundant	3	MGDG 32:5, RT 11.32 min	MGDG 36:5, RT 10.27 min	SQDG 32:2 +3O, RT 12.1 min
106	Less abundant	5	SQDG 30:1 +1O, RT 11.48 min	PC 38:8, RT 11.88 min	SQDG 30:3, RT 9.77 min
			MGDG 34:8, RT 10.15 min	PC 40:4, RT 16.37 min	
107	Less abundant	4	PE 38:7 +3O, RT 7.2 min	SQDG 46:5, RT 15.84 min	PG 42:2 +4O, RT 12.34 min
			DGDG 44:11 +1O, RT 13.32 min		
108	Less abundant	5	PE 38:0, RT 12.66 min	SQDG 38:0 +1O, RT 16.71 min	MGDG 28:4, RT 9.99 min
			PC 36:7, RT 11.45 min	SQDG 44:6, RT 14.99 min	

109	Less abundant	3	SQDG 36:0, RT 15.61 min	PC 32:4, RT 11.64 min	DGDG 50:3 +3O, RT 17.57 min
110	Less abundant	1	SQDG 32:2 +1O, RT 11.89 min	SQDG 32:2 +1O, RT 11.89 min	SQDG 32:2 +1O, RT 11.89 min
			SQDG 32:2 +1O, RT 11.89 min		
111	Less abundant	6	PC 30:3, RT 11.33 min	PC 42:3, RT 17.47 min	PE 44:4 +2O, RT 18.66 min
			TAG 38:1 +1O, RT 16.61 min	PC 38:6 +1O, RT 10.61 min	PE 44:0 +4O, RT 11.06 min
112	Less abundant	3	PC 40:5, RT 11.33 min	PE 36:7, RT 11.57 min	PC 32:3, RT 12.46 min
113	Less abundant	3	SQDG 30:0 +1O, RT 13.82 min	PE 32:0 +2O, RT 12.31 min	DGTS_DGTA 38:9, RT 11.34 min
114	Less abundant	2	SQDG 32:0, RT 13.39 min	SQDG 32:0, RT 13.39 min	SQDG 32:0, RT 13.39 min
			SQDG 32:0, RT 13.39 min	SQDG 30:2, RT 10.32 min	
115	Less abundant	4	SQDG 44:2 +1O, RT 16.36 min	PC 40:9 +1O, RT 9.59 min	SQDG 38:0 +1O, RT 16.74 min
			MGDG 36:7, RT 12.18 min		
116	More abundant	4	SQDG 44:5, RT 15.84 min	PE 44:7 +2O, RT 12.73 min	PE 40:8 +3O, RT 7.54 min
			DGTS_DGTA 38:10, RT 10.71 min		
117	More abundant	4	PC 42:8, RT 14.14 min	DGTS_DGTA 38:2, RT 16.85 min	SQDG 40:5, RT 13.64 min
			DGDG 32:3, RT 12.1 min		
118	More abundant	7	DGDG 32:0, RT 15.07 min	DGDG 50:2 +3O, RT 17.84 min	PE 44:3 +4O, RT 9 min
			DGTS_DGTA 38:7, RT 13.09 min	TAG 48:5 +3O, RT 16.34 min	PC 40:4, RT 12.17 min
			SQDG 48:6 +1O, RT 16.14 min		
119	More abundant	3	PE 32:5 +1O, RT 7.21 min	PC 38:2, RT 16.61 min	TAG 64:14 +4O, RT 14.55 min
120	More abundant	5	PC 42:6, RT 11.79 min	DGDG 38:6, RT 13.34 min	SQDG 34:2, RT 12.62 min
			PE 42:11 +2O, RT 9.79 min	SQDG 36:7, RT 9.89 min	
121	More abundant	3	PC 44:11 +4O, RT 9.67 min	PE 36:6, RT 12.51 min	PG 44:8 +4O, RT 18.66 min
122	More abundant	4	DGDG 32:2, RT 13.09 min	TAG 38:3, RT 14.54 min	DGDG 36:8, RT 10.57 min
			DGTS_DGTA 40:3, RT 16.9 min		
123	More abundant	5	TAG 36:0, RT 17.35 min	TAG 40:1 +1O, RT 16.86 min	DGDG 36:1, RT 16.39 min
			SQDG 28:0, RT 10.99 min	PC 42:5, RT 16.59 min	
124	NS	2	TAG 58:13 +4O, RT 16.23 min	TAG 58:13 +4O, RT 16.23 min	TAG 58:13 +4O, RT 16.23 min
			TAG 58:13 +4O, RT 16.23 min	DGDG 36:7 +4O, RT 12.28 min	
125	More abundant	4	DGTS_DGTA 32:6, RT 10.28 min	TAG 56:13 +4O, RT 16.21 min	PC 30:1, RT 13.03 min

			PC 46:8, RT 17.28 min		
126	More abundant	1	PE 34:6 +1O, RT 7.54 min	PE 34:6 +1O, RT 7.54 min	PE 34:6 +1O, RT 7.54 min
			PE 34:6 +1O, RT 7.54 min		
127	More abundant	5	TAG 48:4 +3O, RT 16.83 min	DGTS_DGTA 44:6, RT 16.76 min	SQDG 34:2, RT 12.65 min
			PE 46:2 +4O, RT 10.55 min	TAG 66:18 +1O, RT 14.27 min	
128	NS	2	SQDG 38:1 +1O, RT 13.09 min	SQDG 38:1 +1O, RT 13.09 min	SQDG 38:1 +1O, RT 13.09 min
			SQDG 38:1 +1O, RT 13.09 min	SQDG 36:1, RT 14.78 min	
129	More abundant	5	PC 38:2, RT 12.89 min	SQDG 34:1, RT 13.62 min	TAG 38:3 +1O, RT 13.15 min
			PE 34:3, RT 13.63 min	PC 34:8, RT 10.74 min	
130	More abundant	3	MGDG 36:9 +3O, RT 9.19 min	PC 40:8, RT 13.05 min	DGDG 50:2 +3O, RT 17.85 min
131	More abundant	4	DGDG 42:4 +3O, RT 15.92 min	MGDG 32:7, RT 6.94 min	PG 44:6 +4O, RT 19.74 min
			PC 36:6 +1O, RT 9.53 min		
132	More abundant	3	DGDG 42:5 +3O, RT 15.46 min	PC 46:6, RT 17.42 min	TAG 46:8 +1O, RT 13.68 min
133	More abundant	4	MGDG 28:0 +3O, RT 13.49 min	PC 46:8, RT 12.75 min	DGTS_DGTA 36:6, RT 12.89 min
			DGCC 34:4 +4O, RT 16.22 min		
134	More abundant	6	SQDG 34:1 +3O, RT 12.86 min	DGDG 36:6, RT 12.17 min	TAG 56:13 +4O, RT 16.23 min
			PE 40:10 +2O, RT 9.35 min	DGDG 38:7, RT 12.41 min	PE 36:5, RT 13.53 min
135	More abundant	3	PC 32:4, RT 13.02 min	PE 38:3 +2O, RT 12.22 min	DGDG 44:2 +3O, RT 16.99 min
136	More abundant	5	PE 40:5 +2O, RT 11.83 min	SQDG 30:4, RT 9.11 min	PC 36:5 +1O, RT 10.3 min
			DGDG 40:2, RT 16.89 min	PC 32:1, RT 14.34 min	
137	More abundant	6	DGTS_DGTA 50:4, RT 19.16 min	SQDG 36:2, RT 13.76 min	SQDG 42:4, RT 15.61 min
			DGTS_DGTA 30:2, RT 12.51 min	PE 44:1 +2O, RT 16.8 min	SQDG 38:0 +1O, RT 14.11 min
138	More abundant	3	PE 42:9, RT 13.25 min	MGDG 42:10 +3O, RT 14.49 min	PC 40:3, RT 13.08 min
139	More abundant	3	TAG 56:10 +4O, RT 16.34 min	PE 38:7, RT 12.75 min	TAG 40:1 +2O, RT 16.52 min
140	More abundant	4	DGDG 40:3 +3O, RT 15.8 min	SQDG 42:4, RT 15.63 min	PE 42:6 +2O, RT 12.27 min
			SQDG 34:5, RT 10.4 min		
141	Less abundant	5	SQDG 36:4 +3O, RT 12.75 min	PE 42:11, RT 12.17 min	PC 44:6, RT 16.68 min
			DGTS_DGTA 46:7, RT 16.9 min	DGTS_DGTA 32:3, RT 12.86 min	
142	NS	2	PC 24:2, RT 11.44 min	PC 24:2, RT 11.44 min	PC 24:2, RT 11.44 min

			PC 24:2, RT 11.44 min	PE 46:4 +4O, RT 9.54 min	
143	NS	4	PE 28:2 +1O, RT 7.2 min	DGDG 36:7, RT 11.23 min	PC 40:2, RT 17.37 min
			PE 32:1, RT 14.46 min		
144	Less abundant	1	SQDG 32:1, RT 12.41 min	SQDG 32:1, RT 12.41 min	SQDG 32:1, RT 12.41 min
			SQDG 32:1, RT 12.41 min		
145	Less abundant	6	DGDG 36:5, RT 13.17 min	MGDG 38:9, RT 7.77 min	PE 34:5, RT 12.21 min
			SQDG 38:2, RT 14.93 min	PE 36:8, RT 10.9 min	SQDG 34:3 +3O, RT 12.36 min
146	NS	2	PC 36:2, RT 11.4 min	PC 36:2, RT 11.4 min	PC 36:2, RT 11.4 min
			PC 36:2, RT 11.4 min	PG 40:0 +2O, RT 10.31 min	
147	NS	2	SQDG 30:0 +1O, RT 12.36 min	SQDG 30:0 +1O, RT 12.36 min	SQDG 30:0 +1O, RT 12.36 min
			SQDG 30:0 +1O, RT 12.36 min	PE 36:3 +2O, RT 11.06 min	
148	Less abundant	4	PE 30:1, RT 13.2 min	PE 42:8, RT 11.68 min	DGTS_DGTA 30:3, RT 11.67 min
			MGDG 36:9, RT 7.11 min		
149	Less abundant	1	PE 32:2, RT 13.42 min	PE 32:2, RT 13.42 min	PE 32:2, RT 13.42 min
			PE 32:2, RT 13.42 min		
150	NS	4	PE 42:3, RT 12.33 min	PE 44:4 +2O, RT 18.66 min	PC 34:0, RT 12.01 min
			DGCC 46:8 +4O, RT 16.41 min		
151	Less abundant	3	DGDG 34:0 +3O, RT 5.68 min	DGTS_DGTA 32:4, RT 12 min	PC 36:6, RT 12.36 min
152	Less abundant	6	PE 36:2 +2O, RT 11.87 min	PE 40:10, RT 12.74 min	PC 30:1 +1O, RT 13.4 min
			SQDG 40:0 +1O, RT 17.51 min	PC 38:10, RT 10.41 min	TAG 34:0, RT 16.85 min
153	Less abundant	6	DGTS_DGTA 36:8, RT 11.04 min	PC 34:4, RT 12.84 min	PG 44:12 +3O, RT 11.5 min
			TAG 38:1 +2O, RT 16.17 min	DGDG 44:11 +1O, RT 13.3 min	PC 38:3, RT 11.79 min
154	NS	2	DGDG 38:3, RT 15.83 min	DGDG 38:3, RT 15.83 min	DGDG 38:3, RT 15.83 min
			DGDG 38:3, RT 15.83 min	PE 38:8, RT 12.03 min	
155	Less abundant	6	PC 28:5 +1O, RT 7.53 min	PE 34:0 +2O, RT 13.51 min	PC 40:10 +1O, RT 9.04 min
			SQDG 32:3, RT 10.66 min	MGDG 34:4, RT 13.56 min	PC 40:5, RT 16.65 min
156	Less abundant	4	SQDG 34:4 +1O, RT 11.5 min	PC 44:7, RT 12.27 min	MGDG 34:5, RT 12.56 min
			SQDG 38:7 +3O, RT 11.5 min		
157	Less abundant	3	PC 42:4, RT 17.13 min	SQDG 40:8 +3O, RT 11.97 min	MGDG 24:1 +4O, RT 6.64 min

158	NS	2	SQDG 34:6, RT 9.53 min	SQDG 34:6, RT 9.53 min	SQDG 34:6, RT 9.53 min
			SQDG 34:6, RT 9.53 min	PE 40:1, RT 13.13 min	
159	Less abundant	4	SQDG 30:0, RT 12.21 min	SQDG 38:1, RT 15.69 min	MGDG 36:9, RT 10.57 min
			SQDG 30:1, RT 11.18 min		
160	Less abundant	3	PC 42:6, RT 15.89 min	PC 32:2, RT 13.29 min	SQDG 32:2, RT 11.43 min
161	Less abundant	4	SQDG 46:5, RT 15.85 min	TAG 42:1 +2O, RT 16.99 min	TAG 64:16 +2O, RT 16.8 min
			PC 40:10, RT 11.5 min		
162	Less abundant	5	DGCC 44:9 +4O, RT 9.05 min	MGDG 48:7 +1O, RT 16.84 min	TAG 54:9 +2O, RT 14.04 min
			PG 48:4 +4O, RT 15.88 min	PC 28:1 +1O, RT 10.9 min	
163	Less abundant	3	MGDG 38:5 +1O, RT 9.9 min	SQDG 40:1 +1O, RT 16.84 min	PG 48:0 +4O, RT 17.42 min
164	Less abundant	5	PE 38:0 +3O, RT 15.02 min	PE 32:1 +2O, RT 9.63 min	PC 46:2, RT 16.79 min
			PG 44:11 +4O, RT 15.57 min	PC 36:4, RT 9.04 min	
165	Less abundant	3	SQDG 34:4 +3O, RT 11.52 min	MGDG 48:4 +1O, RT 17.85 min	PG 44:9 +3O, RT 14.62 min
166	Less abundant	6	MGDG 42:10, RT 10.07 min	MGDG 38:8, RT 11.27 min	SQDG 34:4 +3O, RT 11.57 min
			MGDG 36:10, RT 9.73 min	MGDG 40:9 +1O, RT 11.07 min	PG 48:5 +4O, RT 15.46 min
167	Less abundant	6	MGDG 32:7, RT 9.83 min	MGDG 34:7, RT 10.9 min	PE 34:6 +1O, RT 6.87 min
			SQDG 32:3 +1O, RT 11.03 min	SQDG 36:5 +3O, RT 11.89 min	MGDG 30:2, RT 12.81 min
168	Less abundant	5	PC 38:8 +1O, RT 9.14 min	MGDG 42:8 +1O, RT 9.91 min	PE 38:7, RT 10.17 min
			SQDG 26:3, RT 7.56 min	PG 48:1 +4O, RT 17.1 min	
169	Less abundant	4	MGDG 34:3 +1O, RT 12.4 min	MGDG 34:6, RT 11.6 min	PE 44:6 +1O, RT 12.85 min
			PC 36:3, RT 10.58 min		
170	Less abundant	5	PG 46:1 +4O, RT 16.66 min	PG 48:3 +4O, RT 16.32 min	PE 34:7 +1O, RT 7.26 min
			SQDG 40:3, RT 15.01 min	MGDG 46:2 +1O, RT 18.23 min	
171	Less abundant	3	PE 40:4, RT 13.95 min	PE 38:8 +3O, RT 6.88 min	PC 44:8 +1O, RT 10.01 min
172	Less abundant	4	SQDG 38:0, RT 16.28 min	MGDG 38:8, RT 12.53 min	PC 44:2, RT 15.99 min
			PC 40:3, RT 16.8 min		
173	Less abundant	7	PC 34:6, RT 11.06 min	MGDG 32:6, RT 10.47 min	PE 32:6 +1O, RT 6.88 min
			DGDG 40:7, RT 15.69 min	DGCC 28:0 +4O, RT 6.64 min	PE 44:8 +1O, RT 14.57 min
			MGDG 36:8, RT 7.41 min		

174	Less abundant	4	TAG 54:13 +1O, RT 16.28 min	SQDG 42:3 +3O, RT 10.2 min	PE 38:5 +1O, RT 9.88 min
			SQDG 46:7, RT 15.56 min		
175	Less abundant	7	DGDG 40:8 +1O, RT 15.68 min	MGDG 38:4 +1O, RT 10.63 min	PC 44:7, RT 16 min
			MGDG 48:3 +1O, RT 18.23 min	SQDG 38:3, RT 10.27 min	PE 42:8 +1O, RT 13.77 min
			PE 46:3 +4O, RT 10.02 min		
176	Less abundant	4	MGDG 30:5, RT 10.27 min	SQDG 36:3 +4O, RT 14.6 min	PG 40:3 +4O, RT 10.03 min
			PC 38:9 +1O, RT 8.61 min		
177	Less abundant	3	PE 42:7, RT 13.53 min	MGDG 32:8, RT 9.13 min	MGDG 28:3, RT 10.8 min
178	Less abundant	4	MGDG 38:8, RT 12.55 min	PG 42:4 +4O, RT 10.51 min	MGDG 48:5 +1O, RT 17.56 min
			PE 36:10, RT 9.33 min		
179	Less abundant	4	PE 34:1 +2O, RT 12.5 min	PE 44:1 +4O, RT 10.38 min	PG 44:7 +4O, RT 19.14 min
			MGDG 46:3 +1O, RT 17.8 min		
180	Less abundant	5	MGDG 40:5 +1O, RT 11.18 min	PE 34:9 +4O, RT 8.82 min	MGDG 48:5 +1O, RT 17.51 min
			MGDG 40:7 +1O, RT 10.74 min	PC 42:10 +1O, RT 10.02 min	
181	Less abundant	6	PC 48:8 +4O, RT 7.7 min	DGDG 46:8 +3O, RT 15.26 min	SQDG 36:6 +3O, RT 11.04 min
	Less abundant		PC 44:4, RT 14.48 min	PE 48:4 +4O, RT 10.5 min	MGDG 38:7, RT 13.21 min

[a] Significance at $P \leq 0.01$ determined by two-tailed Student's *t*-test

[b] Difference in abundance between treatments was not significant at $P \leq 0.01$

Table S9. Molecular Characteristics of IPL, ox-IPL, and TAG Observed in *Phaeodactylum tricornutum* after 24 h

Lipid Class or Functional Grouping	Within-Group Mean ± SD		
	Total No. FA Carbon Atoms	Degree Unsaturation	Degree Oxidation[a]
DGCC			
Moieties more abundant[b] (upregulated) under 150 μM H_2O_2 (N = 1)	34	4	4
Moieties less abundant[b] (downregulated) under 150 μM H_2O_2 (N = 4)	39.5 ± 8.1	4.3 ± 4.9	4.0 ± 0.0
DGDG			
Moieties more abundant under 150 μM H_2O_2 (N = 62)	37.2 ± 5.5	4.2 ± 2.7	1.0 ± 1.3
Moieties less abundant under 150 μM H_2O_2 (N = 2)	39.3 ± 6.0	5.5 ± 4.0	1.1 ± 1.1
DGTS & A			
Moieties more abundant under 150 μM H_2O_2 (N = 52)	39.2 ± 4.9	**4.2 ± 2.9**	0.0 ± 0.0
Moieties less abundant under 150 μM H_2O_2 (N = 9)	37.6 ± 5.8	**6.2 ± 2.6**	0.5 ± 0.7
MGDG			
Moieties more abundant under 150 μM H_2O_2 (N = 72)	**38.6 ± 5.3**	**5.2 ± 2.9**	**1.9 ± 1.1*** **
Moieties less abundant under 150 μM H_2O_2 (N = 60)	**37.6 ± 5.8**	**6.2 ± 2.6**	**0.5 ± 0.7*** **
PC			
Moieties more abundant under 150 μM H_2O_2 (N = 92)	38.7 ± 4.5	5.0 ± 3.3	0.4 ± 0.8
Moieties less abundant under 150 μM H_2O_2 (N = 55)	37.6 ± 5.0	5.4 ± 2.6	0.3 ± 0.7
PE			
Moieties more abundant under 150 μM H_2O_2 (N = 68)	**41.1 ± 5.0***	**3.7 ± 3.0**	1.5 ± 1.3
Moieties less abundant under 150 μM H_2O_2 (N = 71)	**38.7 ± 4.8***	**5.1 ± 3.2**	1.3 ± 1.4
PG			
Moieties more abundant under 150 μM H_2O_2 (N = 11)	42.4 ± 2.5	2.1 ± 2.7	3.2 ± 1.0
Moieties less abundant under 150 μM H_2O_2 (N = 21)	42.7 ± 4.9	3.8 ± 4.0	3.5 ± 1.0
SQDG			
Moieties more abundant under 150 μM H_2O_2 (N = 49)	37.2 ± 4.9	2.9 ± 1.9	1.0 ± 1.2
Moieties less abundant under 150 μM H_2O_2 (N = 62)	36.0 ± 5.7	2.8 ± 2.5	1.3 ± 1.4
TAG			
Moieties more abundant under 150 μM H_2O_2 (N = 164)	50.1 ± 7.1	5.6 ± 4.4	**0.9 ± 1.2**
Moieties less abundant under 150 μM H_2O_2 (N = 21)	51.9 ± 13	7.3 ± 6.1	**1.5 ± 1.0**
Chloroplast lipids (DGDG, SQDG, MGDG, PG)			
Moieties more abundant under 150 μM H_2O_2 (N = 194)	38.0 ± 5.3	4.1 ± 2.8	1.5 ± 1.3
Moieties less abundant under 150 μM H_2O_2 (N = 165)	37.8 ± 6.0	4.5 ± 3.3	1.2 ± 1.5
Endoplasmic reticulum lipids (PC, PE, PG)			
Moieties more abundant under 150 μM H_2O_2 (N = 171)	39.9 ± 4.8	4.3 ± 3.2	1.0 ± 1.3
Moieties less abundant under 150 μM H_2O_2 (N = 147)	38.9 ± 5.1	5.0 ± 3.1	1.3 ± 1.5
Mitochondrial lipids (PE, PG)			
Moieties more abundant under 150 μM H_2O_2 (N = 79)	**41.3 ± 4.8**	**3.5 ± 3**	1.7 ± 1.4
Moieties less abundant under 150 μM H_2O_2 (N = 92)	**39.6 ± 5.1**	**4.8 ± 3.4**	1.8 ± 1.6
Betaine lipids (DGCC, DGTS & A)			
Moieties more abundant under 150 μM H_2O_2 (N = 53)	39.1 ± 4.9	4.2 ± 2.9	0.1 ± 0.5
Moieties less abundant under 150 μM H_2O_2 (N = 13)	38.2 ± 6.3	5.5 ± 3.2	1.2 ± 1.9

All lipids			
Moieties more abundant under 150 μM H_2O_2 (N = 571)	**42.1 ± 7.7*** **	4.6 ± 3.5	1.0 ± 1.3
Moieties less abundant under 150 μM H_2O_2 (N = 325)	**38.9 ± 7.2*** **	5.0 ± 3.5	1.1 ± 1.4

For each lipid class or lipid functional grouping, we report the number (N) and mean (± SD) molecular characteristics of those moieties more and less abundant (up- and downregulated) in the 150 μM H_2O_2 treatment after 24 h, compared to the 0 μM H_2O_2 control. A two-tailed Student's *t*-test was used to determine the significance of differences in mean values between groups; differences were significant at $P \leq 0.05$ (bold), $P \leq 0.01$ (*), $P \leq 0.001$ (**), and $P \leq 0.0001$ (***). Data are presented for a single experiment with two technical replicates.

[a] Number of additional oxygen atoms

[b] Compared to 0 μM H_2O_2 control at 24 h

Chart S1. Examples of Isomer and Isobar Annotation from the *P. tricornutum* Dataset

			Database Assignments Applied by LOBSTAHS				
Situation	Diagnostic Code(s) Applied[a]	*m/z* and Corrected RT(s) of Observed Feature	Parent Compound	Adduct	Calculated *m/z* of Adduct Ion	Relative Mass Uncertainty of Match (ppm)	Possible Molecular Structure[b]
Dominant adducts of two different compounds are functional structural isomers	C3f	748.5936 15.7 min	TAG 38:0 +4O	$[M+NH_4]^+$	748.5933	-0.4	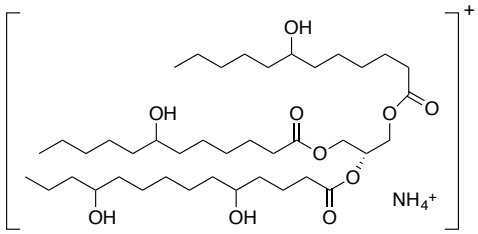
			MGDG 32:0	$[M+NH_4]^+$	748.5933	-0.4	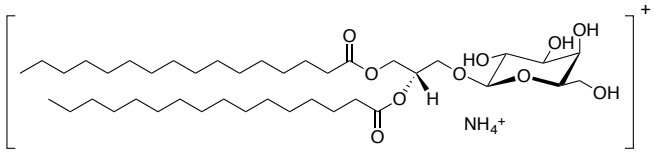
Dominant adducts of two different compounds are isobaric[c]	C3c	808.6080 13.5 min	PE 38:0 +2O	$[M+H]^+$	808.6062	-2.3	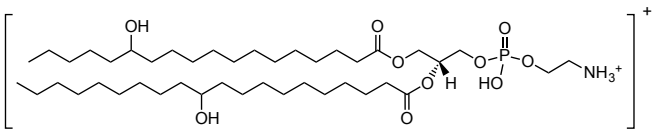
			DGTS 40:8	$[M+H]^+$	808.6086	0.7	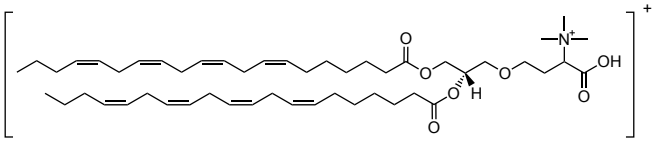
Dominant adducts of different compounds are	C3c, C3f	894.6809 14.9 min	PC 40:0 +3O	$[M+H]^+$	894.6794	-1.7	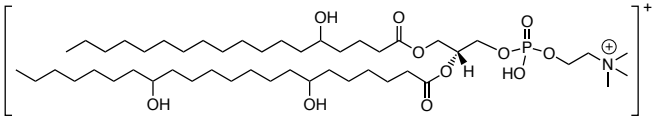

both functional structural isomers and isobaric			PG 42:1 +1O	$[M+NH_4]^+$	894.6794	-1.7	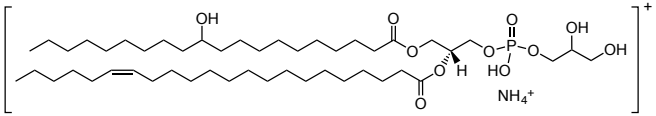
			TAG 52:9 +2O	$[M+NH_4]^+$	894.6818	1.0	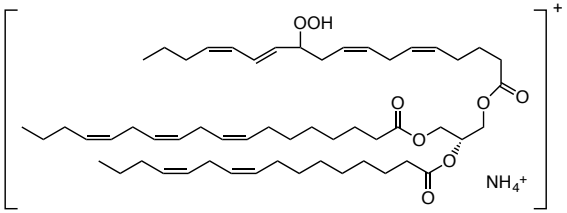
Multiple regioisomers possible for a given compound assignment[d]	C3r	804.5767 13.4 min, 13.1 min	PE 38:2 + 2O	$[M+H]^+$	804.5749	-2.2	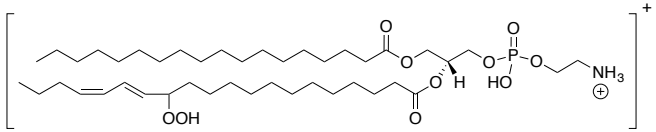
							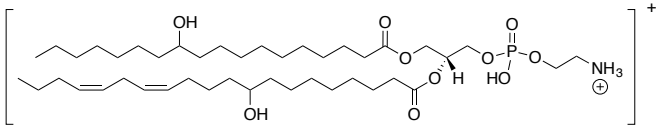

[a] As described in Scheme 1.

[b] Several possible structures can be described by a given parent compound assignment; one possible structure for each assignment is shown in the table.

[c] In this case, the theoretical masses of the two ions were indistinguishable at the ppm (2.5) used database matching.

[d] Inferred from the appearance at different retention times in the same sample of multiple features with the same mass.

REFERENCES USED IN SUPPORTING INFORMATION

(1) Kessner, D.; Chambers, M.; Burke, R.; Agus, D.; Mallick, P. *Bioinformatics* **2008**, *24*, 2534–2536.

(2) Yang, J.; Schmelzer, K.; Georgi, K.; Hammock, B. D. *Anal. Chem.* **2009**, *81*, 8085-8093.

(3) Göbel, C.; Feussner, I. *Phytochemistry* **2009**, *70*, 1485-1503.

(4) Gaquerel, E.; Kuhl, C.; Neumann, S. *Metabolomics* **2013**, *9*, 904-918.

(5) Wolf, S.; Schmidt, S.; Muller-Hannemann, M.; Neumann, S. *BMC Bioinformatics* **2010**, *11*, 148.

(6) van den Berg, R. A.; Hoefsloot, H. C.; Westerhuis, J. A.; Smilde, A. K.; van der Werf, M. J. *BMC Genomics* **2006**, *7*, 142.

(7) Warnes, G. R.; Bolker, B.; Bonebakker, L.; Gentleman, R.; Huber, W.; Liaw, A.; Lumley, T.; Maechler, M.; Magnusson, A.; Moeller, S.; Schwartz, M.; Venables, B. gplots: Various R Programming Tools for Plotting Data. **2016**, R package version 3.0.1.

(8) Whitaker, D.; Christman, M., clustsig: Significant Cluster Analysis. **2014**, R package version 1.1.

(9) Clarke, K. R.; Somerfield, P. J.; Gorley, R. N. *J. Exp. Mar. Biol. Ecol.* **2008**, *366*, 56-69.

(10) Jouhet, J.; Dubots, E.; Maréchal, E.; Block, M. In *Lipids in Photosynthesis*, Wada, H.; Murata, N., Eds.; Springer Netherlands, 2010, pp 349-372.

(11) Yang, Z.-K.; Niu, Y.-F.; Ma, Y.-H.; Xue, J.; Zhang, M.-H.; Yang, W.-D.; Liu, J.-S.; Lu, S.-H.; Guan, Y.; Li, H.-Y. *Biotechnology for Biofuels* **2013**, *6*, 67.

(12) Lesser, M. P. *Annu. Rev. Physiol.* **2006**, *68*, 253-278.

(13) Gill, S. S.; Tuteja, N. *Plant Physiol. Biochem.* **2010**, *48*, 909-930.

(14) Buseman, C. M.; Tamura, P.; Sparks, A. A.; Baughman, E. J.; Maatta, S.; Zhao, J.; Roth, M. R.; Esch, S. W.; Shah, J.; Williams, T. D.; Welti, R. *Plant Physiol.* **2006**, *142*, 28-39.

(15) Popendorf, K. J.; Fredricks, H. F.; Van Mooy, B. A. S. *Lipids* **2013**, *48*, 185-195.

(16) Egeland, E. S. In *Phytoplankton Pigments: Characterization, Chemotaxonomy and Applications in Oceanography*, Roy, S.; Llewellyn, C. A.; Egeland, E. S.; Johnsen, G., Eds.; Cambridge University Press: Cambridge, 2011, pp 665-822.

(17) Libiseller, G.; Dvorzak, M.; Kleb, U.; Gander, E.; Eisenberg, T.; Madeo, F.; Neumann, S.; Trausinger, G.; Sinner, F.; Pieber, T.; Magnes, C. *BMC Bioinformatics* **2015**, *16*, 118.

(18) Patti, G. J.; Tautenhahn, R.; Siuzdak, G. *Nat. Protocols* **2012**, *7*, 508-516.

(19) Clasquin, M. F.; Melamud, E.; Rabinowitz, J. D. *Curr Protoc Bioinformatics* **2012**, *37*, 14.11:14.11.11–14.11.23.

(20) Melamud, E.; Vastag, L.; Rabinowitz, J. D. *Anal. Chem.* **2010**, *82*, 9818-9826.